Matter

CellPress
REVIEWS

Review

Breakthroughs in Designing Commercial-Level Mass-Loading Graphene Electrodes for Electrochemical Double-Layer Capacitors

Liang Chang[1] and Yun Hang Hu[1,*]

Since the first exploration of graphene as an electrode material for electrochemical double-layer capacitors (EDLCs) in 2008, great effort has been made to develop high-performance graphene-based electrodes with commercial-level mass loading up to 10 mg/cm^2 or thickness up to 200 μm. However, a thick electrode usually possesses a long diffusion distance for electrolyte ions and a low accessible surface area, leading to gravimetric capacitance degradation, especially at high current density. In recent years, novel techniques have emerged to solve these issues and have brought significant breakthroughs for graphene-based EDLCs. An ultra-high areal capacitance (>2 F/cm^2) has been achieved at a large graphene mass loading (>10 mg/cm^2) without sacrificing gravimetric capacitance. This article reviews this recent significant progress and emphatically discusses challenges and strategies for highly efficient graphene electrodes to achieve high values for three types of capacitance (gravimetric, volumetric, and areal) at commercial-level mass loadings from the viewpoint of materials design.

Introduction

Clean and renewable energies are expected to satisfy energy demands for the increasing population and to solve environmental issues caused by fossil fuel economies. However, renewable energy sources (such as wind, solar, and geothermal) are all intermittent and generally dispersed. Their efficient use requires reliable energy-storage systems.[1–3] Electrochemical double-layer capacitors (EDLCs), which represent one type of essential energy-storage device, possess fast charge/discharge rate, high-power density, ultralong cycle life, simple operation mode, and ease of integration into electronics.[4,5] They have been widely applied for consumer electronics, electric vehicles, industrial instruments, and new-type grids.[6,7]

EDLCs store energies by forming electrochemical double layers (EDL) at the electrode-electrolyte interface, which requires large surface areas of electrode materials for charge storage.[8–10] However, activated carbon (AC) with large surface area, a common electrode material for EDLCs, cannot provide high capacitance and a satisfactory rate performance, because electrolyte ions are difficult to transport into its rich micropores.[11–14] Therefore, ideal electrode materials for EDLCs would have optimal pore-size distribution that can ensure electrolyte ions to easily diffuse into all pores, leading to a large accessible surface area. The electrode materials of EDLCs should also possess suitable conductivity for electron transfer.[15–18] Graphene, the youngest allotrope of carbon produced and isolated in 2004,[19] is a single-atom-thick carbon sheet with large theoretical surface area (2,630 m^2/g), high carrier mobility (up to 10,000–20,000 cm^2/V/s), and high chemical stability.[20–23] The combination of fully accessible surface area and high conductivity makes graphene an ideal electrode material with a high theoretical capacitance of

Progress and Potential

Electrochemical double-layer capacitors (EDLCs), a type of energy-storage device with second-level energy storage and delivery rate, are widely applied in the field of consumer electronics, electric vehicles, industrial power quality, and new-grid field. EDLCs are experiencing a 20% annual growth, which will reach a market of $2.18 billion in 2020. Currently the EDLC research and industrial efforts focus on development of highly efficient graphene electrodes. To reduce the gap between the research results and the commercial requirements, excellent performance of graphene-based EDLCs must be obtained with a commercial-level mass loading (10 mg/cm^2) of graphene. Over the past 5 years, breakthroughs have been reported for graphene-based EDLCs, achieving ultrahigh areal capacitances (>2 F/cm^2) at a large graphene mass loading (>10 mg/cm^2) without sacrificing gravimetric and volumetric capacitances. These findings are heralding a bright future for EDLCs.

526 F/g for EDLCs, which has stimulated intensive research on graphene-based supercapacitors.[24–27] So far, numerous reviews have been published assessing progress on the application of graphene in EDLCs.[3–5,24,26–30] However, scaling up graphene electrodes to commercial-level mass loading was seldom evaluated in these articles. In this review, from a materials design point of view, we discuss research efforts and highlight the recent breakthroughs for graphene-based EDLCs with emphasis on challenges and strategies in the development of commercial-scale graphene electrodes.

Research Progress in Graphene-Based EDLCs

The research on graphene in supercapacitors started in 2008.[31–33] Rao and coworkers successfully synthesized graphene materials with surface areas of 925 m^2/g by exfoliation of graphitic oxide (EG), which exhibited gravimetric capacitance of 117 F/g in an aqueous H_2SO_4. Ruoff et al. created chemically modified graphene (CMG) with Hummers' method, which possesses large surface area (705 m^2/g) and high conductivity (2×10^2 S/m). The supercapacitor with CMG electrodes achieved a gravimetric capacitance of 135 F/g at current of 10 mA in 5.5 M KOH. Without eliminating the contribution from functional groups, the normalized capacitances for EG and CMG were 12.4 and 19.1 $\mu F/cm^2$, respectively. They are still lower than the intrinsic capacitance of graphene (21 $\mu F/cm^2$), which was directly measured in a three-electrode configuration (Figures 1A and 1B).[34] In the measurement, single-layer graphene as a working electrode was covered by a thick photoresist layer with a 10-nm-diameter window opened for electrolyte exposure, which minimized the background capacitance and prevented exposure of the graphene edges. Such an ideal graphene sheet with surface area of 2,630 m^2/g would possess an EDL capacitance of 526 F/g. However, in EDLCs tests the obtained capacitance of graphene is far below the ideal one.[28,29] This could be attributed to several factors. Two-dimensional (2D) graphene sheets tend to agglomerate and restack in the process of slurry-type electrode fabrication due to strong van der Waals interactions. These can lead to the severe reduction of surface area and the difficult diffusion of electrolyte ions between sheets, causing the deterioration of EDL performance especially at high-rate and high-power conditions.[30,39] Furthermore, the conductivity of graphene electrode could be decreased by defects and functional groups introduced during its top-down synthesis.[40–42]

Recent development of graphene-based EDLCs focuses on creating novel graphene frameworks. One of strategies is to generate pores in graphene sheets.[35,43–47] For example, Zhu et al. activated microwave-exfoliated graphene oxide (a-MEGO) by KOH to form 0.5- to 6-nm-wide pores in sheets (Figure 1C), achieving a surface area up to 3,100 m^2/g and thus a high capacitance of 165 F/g at 1.4 A/g with electrolyte of 1-butyl-3-methyl-imidazolium tetrafluoroborate.[35] The construction of a restacking-inhibited structure (composed of intersheet meso- and macropores) is another strategy. Shi and coworkers hydrothermally synthesized self-assembled graphene hydrogel (SGH) (Figure 1D), in which graphene sheets overlapped and coalesced to form a well-defined and interconnected three-dimensional (3D) porous network (Figure 1E).[36] The SGH exhibited a capacitance of 175 F/g in 5 M KOH due to the increase of surface area and ion transport. These graphene hydrogels/aerogels can be modified for flexible supercapacitors[48,49] or be further decorated with pseudo-atoms (O, N, S) (or transition metal oxides) for pseudo-/hybrid capacitors.[39,50–53] However, defects in graphene oxide (GO) and reduced GO (rGO) with large quantity brought a negative impact on conductivity and thus the capacitive performance. This issue was solved by 3D graphene foams, which were synthesized by Cheng and coworkers with the template-directed chemical vapor deposition technique (Figures 1F and 1G).[37] This bottom-up strategy generated high-quality three-layer graphene sheets

[1]Department of Materials Science and Engineering, Michigan Technological University, 1400 Townsend Drive, Houghton, MI 49931-1295, USA

*Correspondence: yunhangh@mtu.edu

https://doi.org/10.1016/j.matt.2019.06.016

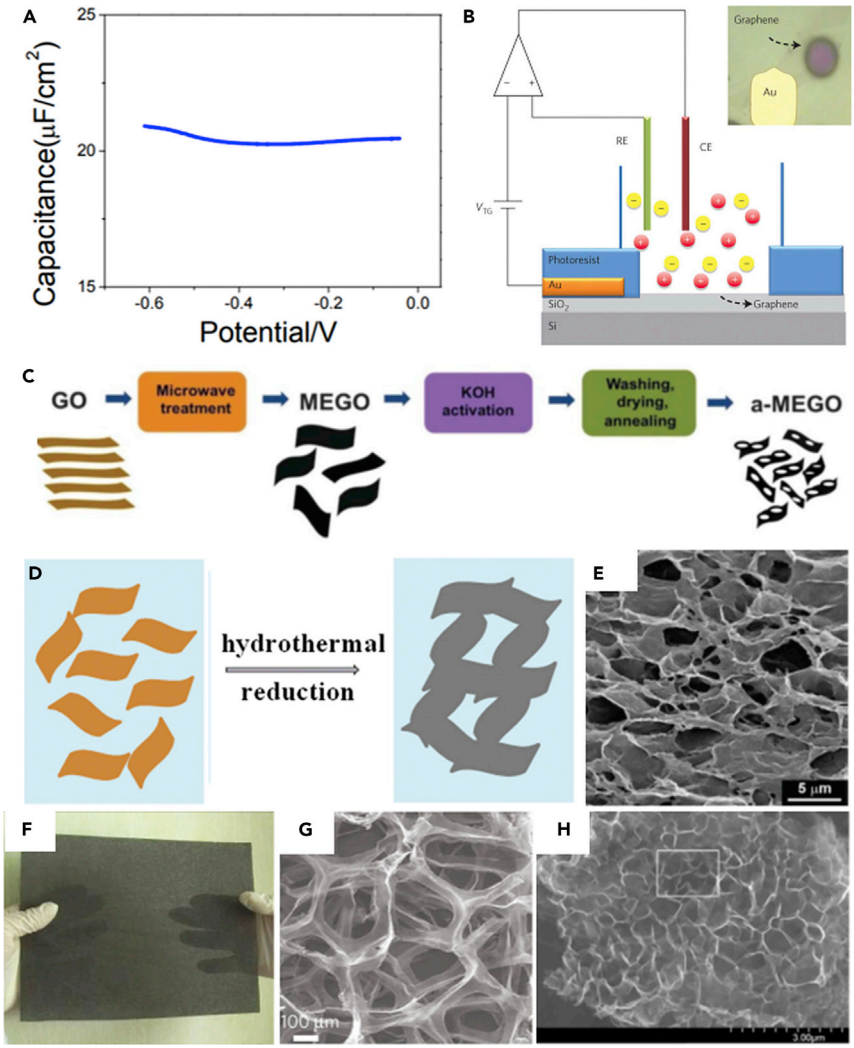

Figure 1. Progress of Graphene-Based EDLCs

(A) Double-layer capacitance versus gate potential in [BMIM]PF_6/Pt interface.

(B) Single-layer graphene device. Reprinted by permission from Springer Customer Service Center GmbH: Springer Nature, *Nature Nanotechnology*, Xia et al.,[34] Copyright 2009.

(C) Schematic showing the microwave exfoliation/reduction of GO and the following chemical activation of MEGO with KOH. From Zhu et al.[35] Reprinted with permission from AAAS.

(D) The proposed formation mechanism for SGH.

(E) Scanning electron microscopy (SEM) image of the SGH interior microstructures. Reprinted with permission from Xu et al.[36] Copyright 2010, American Chemical Society.

(F) Photograph of a 170 × 220-mm^2 free-standing graphene foam.

(G) SEM image of a graphene foam. Reprinted by permission from Springer Customer Service Center GmbH: Springer Nature, *Nature Materials*, Chen et al.,[37] Copyright 2011.

(H) SEM images of honeycomb-structured graphene.

Adapted with permission from Wang et al.[38] Copyright 2013, Wiley-VCH Verlag GmbH & Co. KGaA, Weinheim.

with excellent connection in three dimensions, leading to large surface area and high electrical conductivity. Furthermore, new chemistry and new procedures emerged for constructing 3D graphene with various shapes (Figure 1H), such as the reaction of alkali metals with carbon oxides to 3D graphene, which exhibited excellent performance for EDLCs due to their large accessible surface area and high electrical conductivity.[38,54–57]

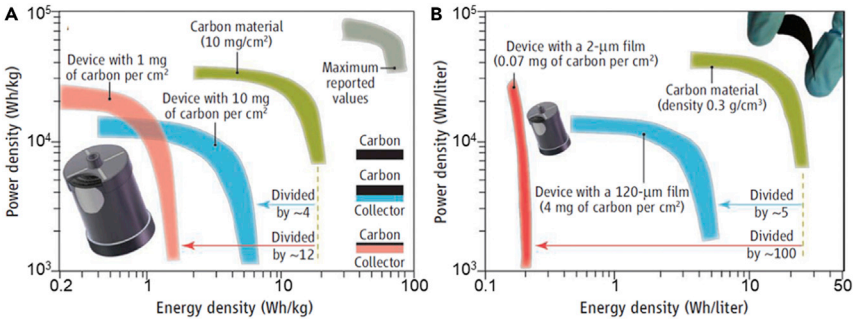

Figure 2. A Tale of Two Plots

One way to compare electrochemical energy-storage devices is to use Ragone plots, which show both power density (speed of charge and discharge) and energy density (storage capacity). These plots for the same EDLCs are on a gravimetric (per weight) basis in (A) and on a volumetric basis in (B). The plots show that excellent properties of carbon materials will not translate to medium- and large-scale devices if thin-film and/or low-density electrodes are used. From Gogotsi et al.[70] Reprinted with permission from AAAS.

Other progress was also obtained for graphene electrodes. The relationships between the pore morphology (interface structure, or N-doping induced electronic modification) of graphene materials and their capacitance (charging rate, or ion migration) were revealed by computational simulations.[58–61] Furthermore, the packing density and mass loading of graphene films as well as their areal and volumetric capacitances were recently emphasized for reliable evaluations of graphene electrodes.[62–65]

Challenges in Catering for Commercial Requirements

For commercial applications, an electrode material must store a large amount of charges and rapidly deliver sufficient charges (electrons and ions) in a given charge/discharge duration.[66,67] High energy and power densities require a large surface area for EDL formation and a short electrolyte-ion diffusion distance for rate performance.[68] This is often achieved by a very thin electrode (mass loading <1 mg/cm^2) with a graphene material. However, the excellent gravimetric performance with such a low mass loading is meaningless in practice (Figure 2).[69,70] When the mass loading increases to the commercial level (10 mg/cm^2 or 200 μm thickness),[70] electrochemical performance is significantly influenced by the increased ion-diffusion limitation.[71] This happens because, in an electrode with a high mass loading, gravimetric capacitance can be sustained only when ions and electrons transport across a longer distance at a proportionally high rate.[72] Insufficient charge transfer could bring considerably high outpotential, causing severe capacitance degradation. For this reason, the excellent electrochemical performance (especially the gravimetric-based parameters) achieved at a low mass loading of electrode material cannot be reproduced at a high mass loading.

Ideal electrode materials for commercial supercapacitors must possess not only high gravimetric capacitance but also excellent volumetric and areal ones.[63] However, there is a trade-off relationship among these three types of criteria. Gravimetric performance reflects the energy-storage ability of an electrode material based on how much and how rapidly energy is stored per unit weight. It prefers a thinner electrode. Volumetric performance is determined by energy stored in a unit volume, which shows practical importance for energy-storage devices with limited space. Only electrode materials with high packing density can exhibit a high volumetric

performance. Areal capacitance is energy stored in a unit area, which requires a thicker electrode.[73] Therefore, large gravimetric capacitance demands a highly porous structure of an electrode material to boost its surface area and ion diffusion, whereas high volumetric capacitance prefers a more dense structure.[74,75] Furthermore, high areal capacitance needs to combine a high gravimetric capacitance with a large mass loading. In addition, fast electrolyte-ion transport requires a macro-/mesoporous structure of an electrode.[76,77] In conclusion, the most important consideration for the design and synthesis of graphene electrode materials is to balance two conflicting factors: large density and high porosity.[78,79]

A thick electrode with a large mass loading is more meaningful for practical applications than a thin one. In most academic papers, the claimed specific capacitances, power densities, and energy densities for electrodes are based on active materials in an unpacked configuration. However, in a packed EDLC, the whole weight of the device should be taken into account, including electrode films, current collectors, separators, electrolyte, binder, connectors, and packages. Even if the inference is based on commercial-level mass loading of 10 mg/cm^2, the mass of active materials is only about 30% of the total mass. This indicates that the device performance determined from the electrode property should be divided by 3 or 4.[70] The number would be increased to 30 if a thinner electrode with a mass loading of 1 mg/cm^2 is applied. Therefore, a large mass loading of an electrode is necessary to reduce overheads from other parts, leading to high electrochemical performance for a device.

Strategies for Scalable Graphene Electrodes

Commercialized EDLCs require electrodes with mass loading of 10 mg/cm^2 or thickness about 200 μm, which is remarkably larger than mass loading (usually 1 mg/cm^2 and always below 5 mg/cm^2) reported in most academic papers. As shown in Figure 3, to meet the commercial requirements for EDLC electrodes, the following parameters must be considered for the design and synthesis of ideal electrode materials: large accessible surface areas and fast ion/electron transport pathways in a high packing density form as well as easy scale-up production. Two types of strategies have been developed for ideal graphene electrodes: the reconstruction of 2D graphene as the top-down approach and the direct synthesis of 3D graphene as the bottom-up approach.

Scalable Electrodes Constructed with 2D Graphene

As an effective strategy, 2D graphene can be assembled into macroscale architectures.[80–82] 2D graphene utilized in these processes was synthesized by the chemical oxidation and exfoliation of graphite with the modified Hummers' method. The obtained 2D graphene has advantages of low cost, light weight, excellent flexibility, and high mechanical and chemical stability.[83–86] The graphene without any treatment could reach a high packing density, but suffer severe aggregation during electrode fabrication, causing significant capacitance drop, especially at a high rate with a large mass loading.[87] In contrast, a porous graphene framework, which is obtained by treating the 2D graphene, could exhibit excellent electrochemical performance on the gravimetric scale. For instance, Chen and coworkers synthesized the open-porous and continuously crosslinked rGO foams via a leavening and thermal streaming strategy. The rGO foams, in a two-electrode supercapacitor cell, exhibited a high specific capacitance of 110 F/g, which is much larger than the 17 F/g of rGO films.[81] Qu and coworkers constructed a versatile, ultralight, and nitrogen-doped graphene framework with a pyrrole-assisted hydrothermal method, followed by freeze-drying and Ar-heat treatments. The obtained graphene framework with an ultralow density of 2.1 $\pm$ 0.3 mg/cm^3 was explored for supercapacitor electrodes, reaching 484 F/g

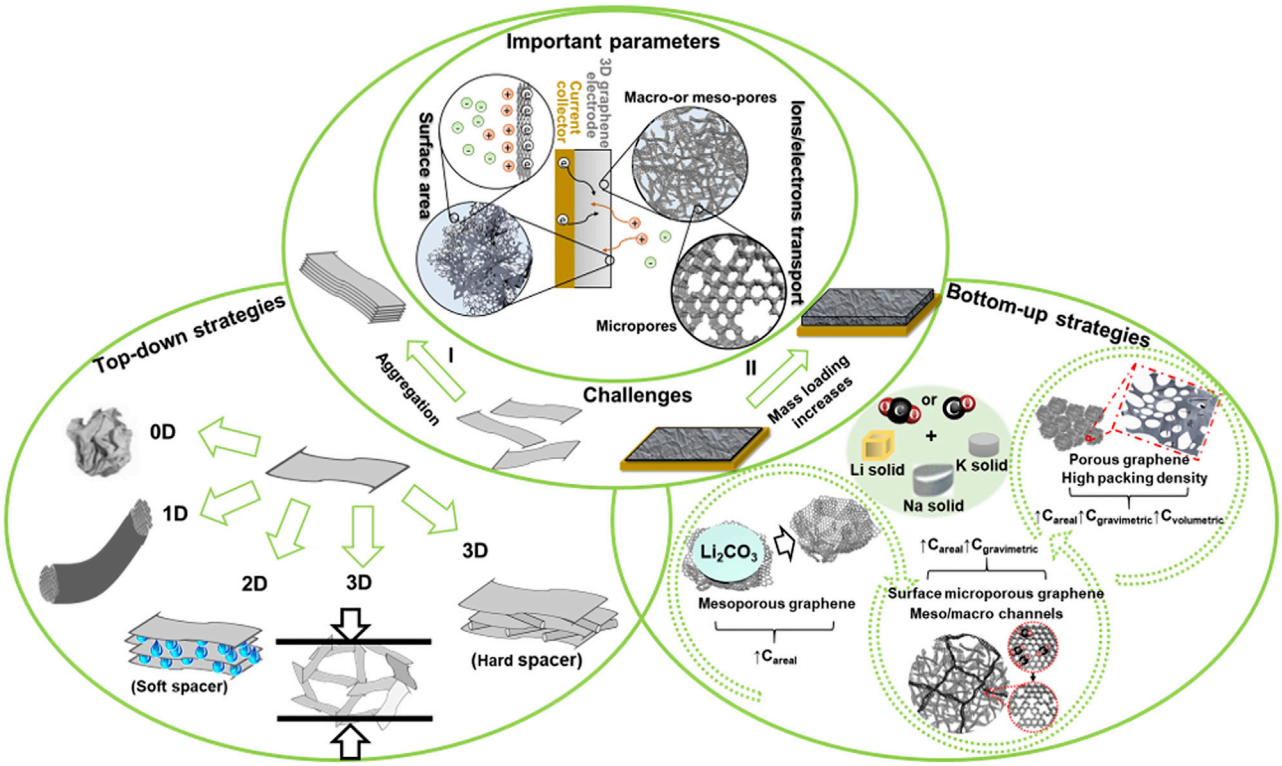

Figure 3. Schematic Illustration
Important parameters, challenges, and synthesis strategies for scalable graphene electrodes.

at 1 A/g in a three-electrode configuration.[82] However, the low packing density led to a low volumetric capacitance and a difficulty for scaling up. To solve these issues, porous but highly dense graphene macroscale architectures were constructed in the forms of graphene balls (zero-dimensional [0D]), graphene fibers (one-dimensional [1D]), graphene papers (2D), compressed graphene hydrogels/aerogels (3D), and graphene/carbon spacer frameworks (3D).

Graphene Balls. The construction of individual graphene sheets to a 0D macroscopic structure was demonstrated as an effective strategy to prevent aggregation of graphene sheets and achieve a high mass loading without capacitance degradation. Luo et al. designed a graphene architecture with a crumpled paper ball structure by isotropic capillary compression, in which the droplets of GO dispersion generated by an aerosol spray pyrolysis step were rapidly evaporated.[88,89] The obtained crumpled rGO balls with a near-spherical contour and a strain-hardening feature can resist more compression than heavily wrinkled graphene sheets with a planer contour (Figures 4A and 4B). This was supported by the change of Brunauer-Emmett-Teller (BET) surface area after being pelletized. Compared with the huge drop from 407 to 66 m^2/g for the wrinkled graphene sheets, the crumpled graphene balls suffered only a relatively small decrease from 567 to 255 m^2/g. This was attributed to the almost unchanged morphology of individual crumpled balls in the compressed pellets and the indistinguishable microstructures of surface and cross-section. Furthermore, the free spaces, which uniformly distribute inside each ball as well as between them, ensure the fast diffusion of ions even for an electrode with a large mass loading. Thus, the crumpled rGO balls can reach an ultrahigh mass loading without obvious decrease in their gravimetric capacitance, namely, its

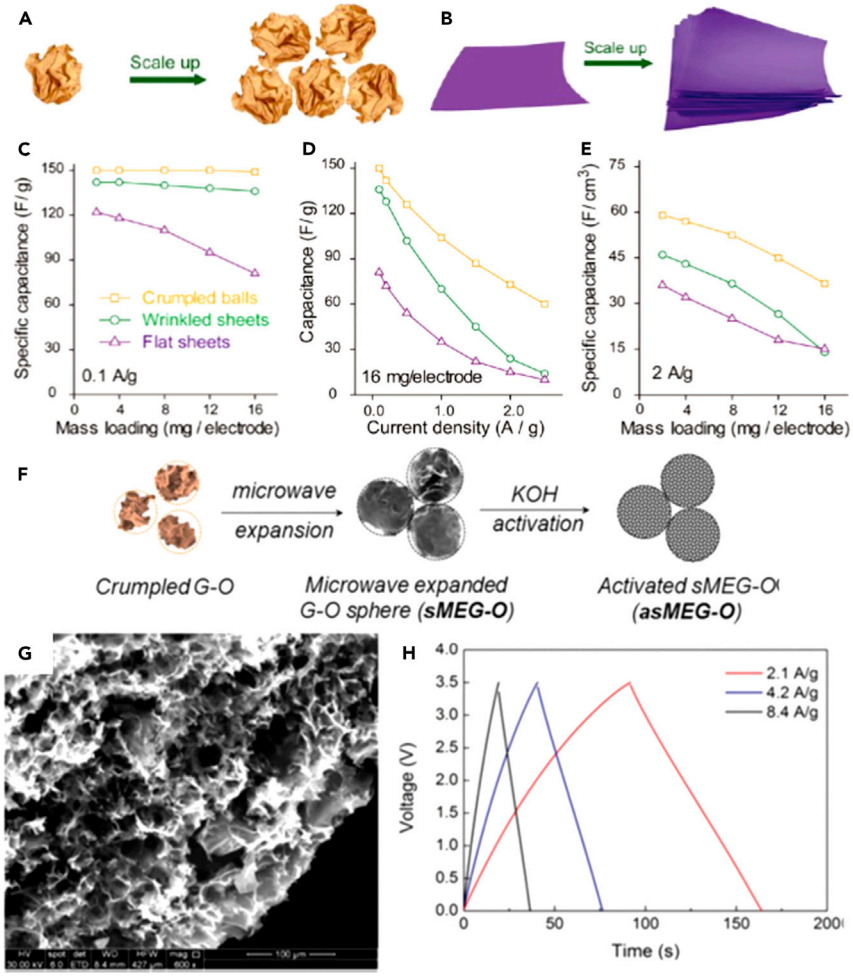

Figure 4. Graphene Balls for EDLC Electrodes

(A and B) Schematic of crumpled graphene balls (A) and flat graphene sheets (B) scaling up.

(C) Mass-based specific capacitance as a function of mass loading at current density of 0.1 A/g.

(D) Mass-based specific capacitance as a function of current density with mass loading of 16 mg/electrode.

(E) Volumetric specific capacitance as a function of mass loading at 2 A/g. Reprinted with permission from Luo et al.[89] Copyright 2013, American Chemical Society.

(F) Schematic of the fabrication of highly porous graphene-derived carbons with hierarchical pore structures.

(G and H) SEM micrograph of asMEG-O (G) and electrochemical characterization of asMEG-O in [EMIM][TFSI]/AN electrolyte (H). Reprinted with permission from Kim et al.[90] Copyright 2013, American Chemical Society.

high gravimetric capacitance of around 150 F/g at 0.1 A/g remained unchanged with increasing mass loading from 2.5 to 20 mg/cm^2 (Figure 4C). However, its performance was greatly affected by a rate (Figure 4D), namely, its areal capacitance decreased from 2.7 to 1.26 F/cm^2 with increasing rate from 0.1 to 2 A/g. Furthermore, its volumetric capacitance is only 58 F/cm^3 due to low density of bulk materials (0.5 g/cm^3) (Figure 4E). To improve rate performance, Kim et al. proposed to graft mesopores within interconnected macroporous frameworks.[90] A microwave treatment was utilized to expand the crumpled balls to a larger volume with some degree of deoxygenation. These microwave-expanded GO balls were infiltrated in a KOH aqueous solution, followed by filtering with vacuum and then thermal activation

under argon flow (Figure 4F). The obtained a-MEGO possessed an open and interconnected macroporous structure (Figure 4G), which was attributed to capillary forces in the self-assembly process of densely packed particles. Furthermore, the KOH activation created a large fraction of micro- and mesopores within the interconnected macroporous network. The a-MEGO had large surface area (3,290 m^2/g) and rich functional groups (2.84 wt % O), providing a large number of active sites for electrolyte ions. Indeed, it exhibited the improved electrochemical performance with capacitance of 174 F/g (or 100 F/cm^3) at 1.1 A/g in an ionic liquid electrolyte (Figure 4H). Although the capacitance value dropped to 129 F/g (or 58 F/cm^3) for a thick electrode (10.4 mg/cm^2 and 230 μm), relatively high volumetric energy density (44 Wh/L) and power density (210 kW/L) were obtained for porous carbon electrodes without any further electrode densification. It is clear that the 0D graphene-based macroscale architecture shows its potential as electrodes of EDLCs to reach the commercial-level mass loading. However, its large resistance of intra- and interparticles greatly limits its rate performance. This stimulated the further modification of graphene balls, such as size and structural control,[91] porous carbon nanotube networks decoration,[92] and metal/metal oxide nanocrystal hybrids,[93–95] which can improve accessible active sites and interparticle conductivity.[96] Nevertheless, the complicated synthetic procedures constrict large-scale application of these 0D graphene-based macroscale architectures.

Graphene Fibers. 1D macroscale architectures of graphene were also explored to reach a large mass loading of 10 mg/cm^2 for scalable graphene electrodes. Graphene fibers (GFs), which possess unique properties of large surface area, high mechanical stability, and excellent electrical and thermal conductivity,[97] have been widely exploited as single-fiber electrodes or parallel pattern electrodes in flexible solid-state micro-supercapacitors[98,99] or graphene-based coaxial fiber supercapacitors.[100,101] However, severe aggregation of graphene sheets in GFs led to a compact structure, inhibiting the transfer of ions and thus decreasing the capacitance. This caused the difficulty for GFs to achieve high specific capacitance per fiber and large areal capacitance per device. An effective strategy was proposed to solve this issue, namely, the ion-diffusion path perpendicular to the fiber's axis was constructed by creating voids between graphene sheets.[102,103] This has created several approaches. Cai et al. selectively adopted a metal needle with concave-convex-shaped inner walls as the spinneret (Figure 5A) to fabricate surface-porous neat graphene fibers (SGF).[104] The nanoscale porous flower structure and impressive surface area of 839 m^2/g allowed SGF to exhibit excellent performance with areal capacitance of 0.23 F/cm^2 at 39.7 mA/cm^2 in a two-electrode micro-supercapacitor. Huang et al. used the repulsive force of water and alcohol molecules to produce porous graphene ribbons (PGRs): the supramolecular hydrogel, which was composed of GO suspension and sodium deoxycholate (NaDC), was electro-spun into ethanol (Figure 5B).[105] The NaDC dissolved into ethanol, whereas water molecules remained inside the frameworks of GO sheets, leading to a porous structure instead of collapsing and restacking. In PGR electrodes, the gel electrolyte was easily infiltrated into the intraspace, and the graphene surface with area of 697 m^2/g was fully utilized. As a result, a high gravimetric capacitance of 208.7 F/g was achieved in a symmetrical-solid-state yarn supercapacitor. This was attributed to porous GFs with continuous ion-diffusion routes on the surface and inside GFs as well as a fast electron transport pathway along the fiber axis. However, its areal capacitance is still far below 0.5 F/cm^2. To conquer this issue, Li and coworkers constructed a new material, hydrothermally activated graphene fiber fabrics (HAGFFs), via the following steps (Figure 5C).[106] A hydrothermal treatment was exploited to partially reduce wet-spun GO fibers into GO/rGO fibers. The partially

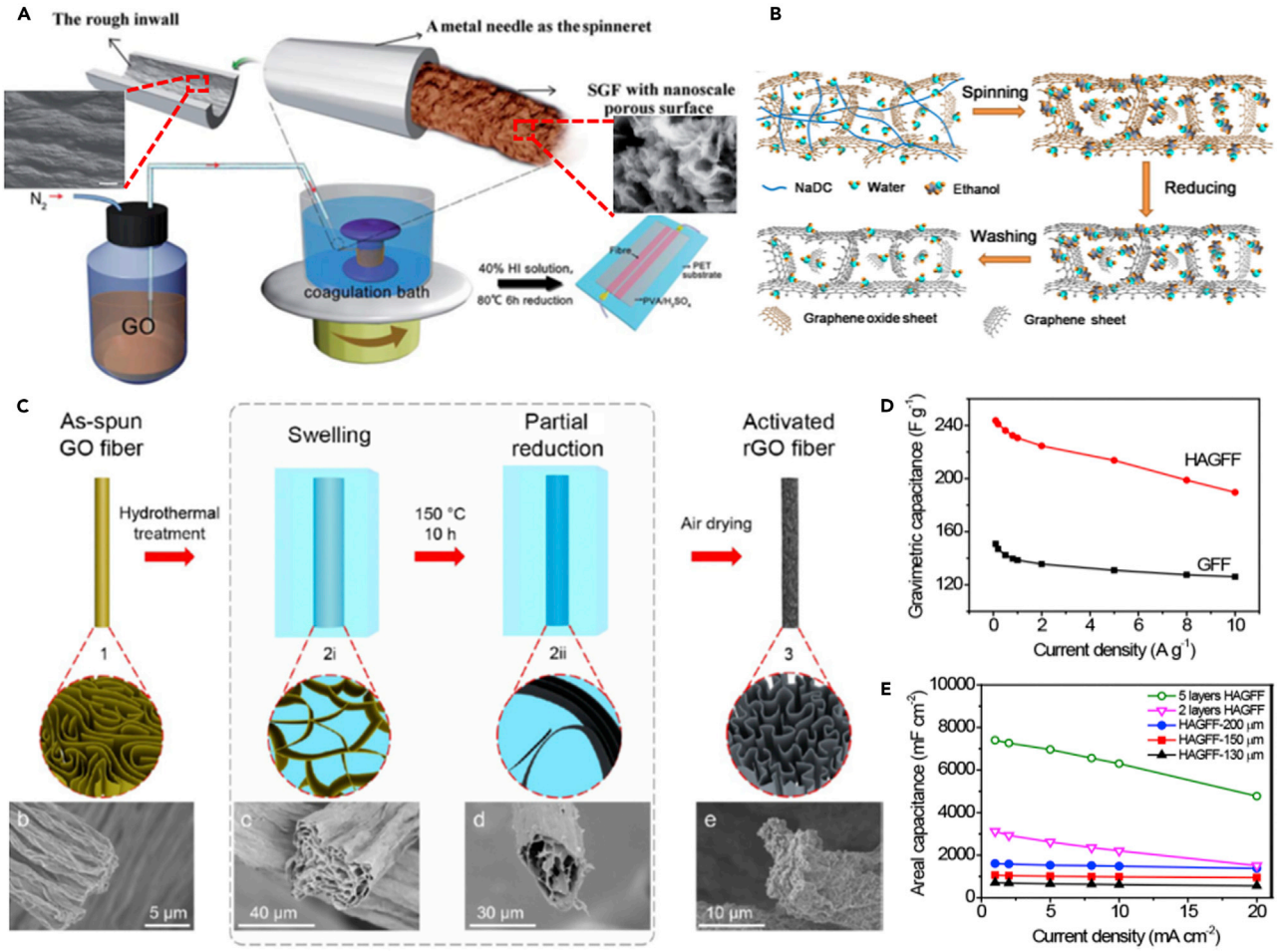

Figure 5. Graphene Fibers for EDLC Electrodes

(A) Wet spinning apparatus for the synthesis of continuous neat graphene fibers and the processing steps for the assembly of flexible solid-state micro-SCs; insets are SEM images of the inner wall of the needle (left) and an SGF electrode (right). Reproduced from Cai et al.,[104] with permission from the Royal Society of Chemistry.

(B) Schematic showing the formation mechanism of the PGRs. Reproduced with permission from Huang et al.[105] Copyright 2015, Elsevier.

(C) The structural evolution of graphene fibers during the hydrothermal activation process. Schematic diagrams with cross-sectional SEM images of graphene fibers in the corresponding stages: (b) as-spun GO fiber, (c) swelled GO gel fiber at the beginning of hydrothermal treatment, (d) rGO gel fiber at the end of hydrothermal treatment, (e) the resulting hierarchical rGO fiber after air-drying.

(D) Calculated gravimetric capacitance of HAGFF and GFF.

(E) Areal capacitance of HAGFF electrodes with various thicknesses.

(C) to (E) reprinted with permission from Li et al.[106] Copyright 2017, American Chemical Society.

reduced GO/rGO microfibers were cut into staples via high-speed shearing in water and then filtered to obtain nonwoven fabrics. The wet products were fully air-dried to form the highly wrinkled microstructures. The obtained HAGFFs possessed special features different from GO fiber fabrics, including high C/O ratio of 4.3, D/G peak intensity ratio of 1.7, increased surface area of 245 m^2/g, concentrated pores below 10 nm, high conductivity of 4 S/m, and improved packing density. This can be explained by the synthetic process. The pre-dried spun GO fibers introduced a compact and lamellar structure. Those hydrophilic fibers, in the initial hydrothermal stage, experienced a thorough swelling once in contact with water, leading to apparently expanded fiber diameter from ~10.7 μm to ~42.5 μm and highly porous inner-fiber structure. The following hydrothermal treatment at 150°C for 10 h decreased electrostatic repulsion and enhanced hydrophobic interactions among

rGO sheets, which made fibers reduced, shrunk, and interfused. Finally, tremendous wrinkles on the rGO sheets and hierarchical morphology of HAGFFs were generated by the air-conditioned drying process. As electrodes for EDLCs, HAGFFs achieved a gravimetric capacitance of 244 F/g and an areal capacitance of 1.06 F/cm^2 with 150 μm-thick films (Figure 5D). If five layers of 200 μm-thick films were overlaid, a record value of 7.40 F/cm^2 was obtained at a rate of 1 mA/cm^2 (Figure 5E). In addition, modification with electrochemical active materials (such as transition metal dichalcogenides or polymers) can further improve the performance of GFs-based supercapacitors.[107–109] As discussed above, the optimizing strategy for the 1D graphene architecture must balance high density and large ion-accessible surface area for efficient mass loading and high areal capacitance.

Graphene Papers. It is well known that graphite-like layer-by-layer assembly is an effective method to achieve high packing density for carbon materials. However, the inevitable aggregation and restacking of 2D graphene due to intersheet van der Waals attractions leads to a multilayer graphene structure behaving as graphite instead of individual graphene. This could cause the loss of accessible surface area and sluggish ion/electron transport, resulting in compromised specific capacitance. To prevent the formation of graphite-like graphene architecture, Li and coworkers created effective spaces for electrolyte-ion transport in the principle of colloid chemistry through a bioinspired strategy.[110] The chemical converted graphene (CCG) hydrogel films (Figure 6A) were synthesized by vacuum filtrating CCG dispersion through a mixed cellulose ester filter membrane and then immersing this product in water overnight. In this process, water was introduced into face-to-face stacked graphene sheets as spacers and created the separation between hydrated CCG sheets (Figures 6B–6D). It was an unusual assembly with a combination of intrinsic corrugation and colloidal interaction between CCG sheets. The obtained self-stacked, solvated graphene (SSG) film was constituted with about 92 wt % water and 0.045 mg/cm^2 CCG, creating high conductivity of 1,860 Ω/sq. The surface accessibility of this SSG film was examined in an aqueous two-electrode supercapacitor. A specific gravimetric capacitance up to 215 F/g was achieved with SSG films and charge/discharge rates were demonstrated to have a negligible effect on energy-storage ability (Figure 6E). However, its low packing density would limit the scaling up of its mass loading to the commercial level. Although the water was removed to enhance the density by a freeze-drying or thermal annealing process, a huge drop in capacitance was observed. This indicates the importance of keeping effective routes for fast diffusion of electrolyte ions during increasing the packing density of the electrode material by removing spacers. For this reason, water was replaced with a ratio-controlled volatile/nonvolatile miscible solution, in which the volatile liquid was water and the nonvolatile liquid was an electrolyte, sulfuric acid or an ionic liquid (1-ethyl-3-methylimidazolium tetrafluoroborate [EMIMBF$_4$]) (Figures 6F–6I).[65] After a simple directional-flow-induced bottom-up assembly process and a capillary compression procedure, a highly porous densely packed carbon material was obtained as electrolyte-mediated chemically converted graphene (EM-CCG). The EM-CCG film with face-to-face stacking realized regulation of packing density by simply controlling the concentration ratios of H_2O/H_2SO_4 or H_2O/EMIMBF$_4$ trapped in a gel, leading to ρ = 1.33, 0.76, 0.42, and 0.13 g/cm^3 for CCG/H_2SO_4 films or ρ = 1.25, 0.97, 0.65, and 0.39 g/cm^3 for CCG/EMIMBF$_4$ films. As a result, only a slight decrease (from 203.7 to 191.7 F/g) in gravimetric capacitance was observed when the packing density increased from 0.13 to 1.33 g/cm^3. Thus, the volumetric capacitance of the EM-CCG films, which was nearly proportional to its packing density, reached the highest value of 261.3 F/cm^3 in EMIMBF$_4$ (Figure 6J) and 255.5 F/cm^3 in H_2SO_4 (Figure 6K). Furthermore, it also exhibited a

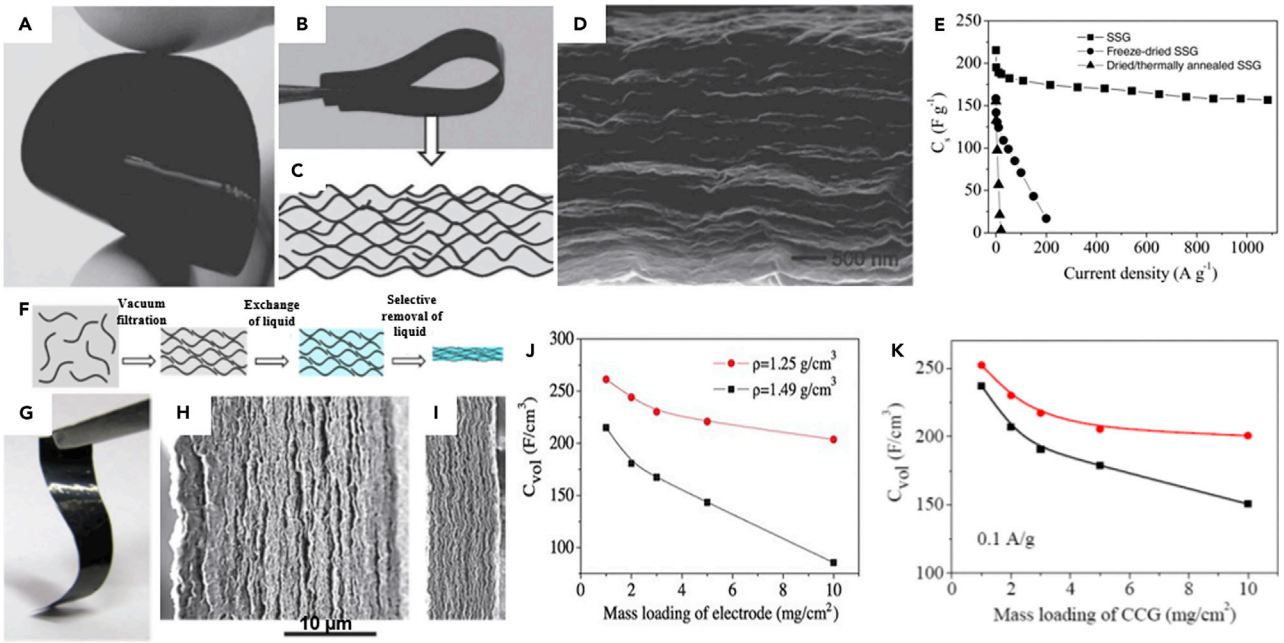

Figure 6. Graphene Papers for EDLC Electrodes

(A and B) Photographs of the as-formed flexible SSG films.

(C) Schematic of the cross-section of the SSG film.

(D) SEM image of the cross-section of a freeze-dried SSG film.

(E) Gravimetric capacitance of SSG, freeze-dried SSG, and dried/thermally annealed SSG measured at various charge/discharge currents. Adapted with permission from Yang et al.[110] Copyright 2011, Wiley-VCH Verlag GmbH & Co. KGaA, Weinheim.

(F) Schematic showing the soft chemistry route to fabricate the EM-CCG film from the CCG dispersion.

(G) A photograph showing the flexibility of EM-CCG film.

(H–K) SEM images of cross-sections of the obtained EM-CCG films containing (H) 78.9 vol % and (I) 27.2 vol % of H_2SO_4, respectively, corresponding to ρ = 0.42 g/cm^3 and ρ = 1.33 g/cm^3, volumetric capacitance as a function of mass loading of EM-CCG film (ρ = 1.25 g/cm^3), and the dried CCG film (ρ = 1.49 g/cm^3) at the current density of 0.1 A/g in ECs with $EMIMBF_4$/AN (J) and in 1.0 M H_2SO_4 (K).

From Yang et al.[65] Reprinted with permission from AAAS.

record volumetric energy density of 59.9 Wh/L. This might be due to its densely packed graphene structure and highly efficient ion transport channels formed by fluid liquid electrolyte. In addition, the EM-CCG film was scaled up to 10 mg/cm^2 and reached a high areal capacitance of 1.57 F/cm^2 in aqueous electrolyte. Therefore, we can conclude that introducing intersheet spacers into graphite-like graphene materials can not only improve the packing density but also enhance the accessible surface area with continuous ion networks, which would benefit gravimetric and areal capacitances as well as volumetric capacitance.

Compressed Graphene Hydrogel/Aerogels. High-force mechanical compression was also exploited to improve the packing density of 3D hydrogel/aerogel, which is a highly interconnected graphene network with exceptional mechanical and electrical robustness (Figure 7A).[49] As an electrode material, 3D hydrogel/aerogel reached a high areal capacitance (0.372 F/cm^2) with an electrode of 185 μm thick (Figures 7B and 7C). However, its low packing density (0.05–2 mg/cm^3) resulted in its small volumetric capacitance and low electrode scalability.[111] Tao et al. employed the evaporation-induced drying technique to post-treat graphene hydrogels with a low density of 0.02 g/cm^3, forming a novel high-density porous graphene macroform (HPGM).[112] In this process, graphene nanosheets were effectively interlinked to construct 3D hydrogel and the parent hydrogel shrunk to about one-eighth of volume after removing water. As a result, the obtained HPGM possessed a compact microstructure with closely and

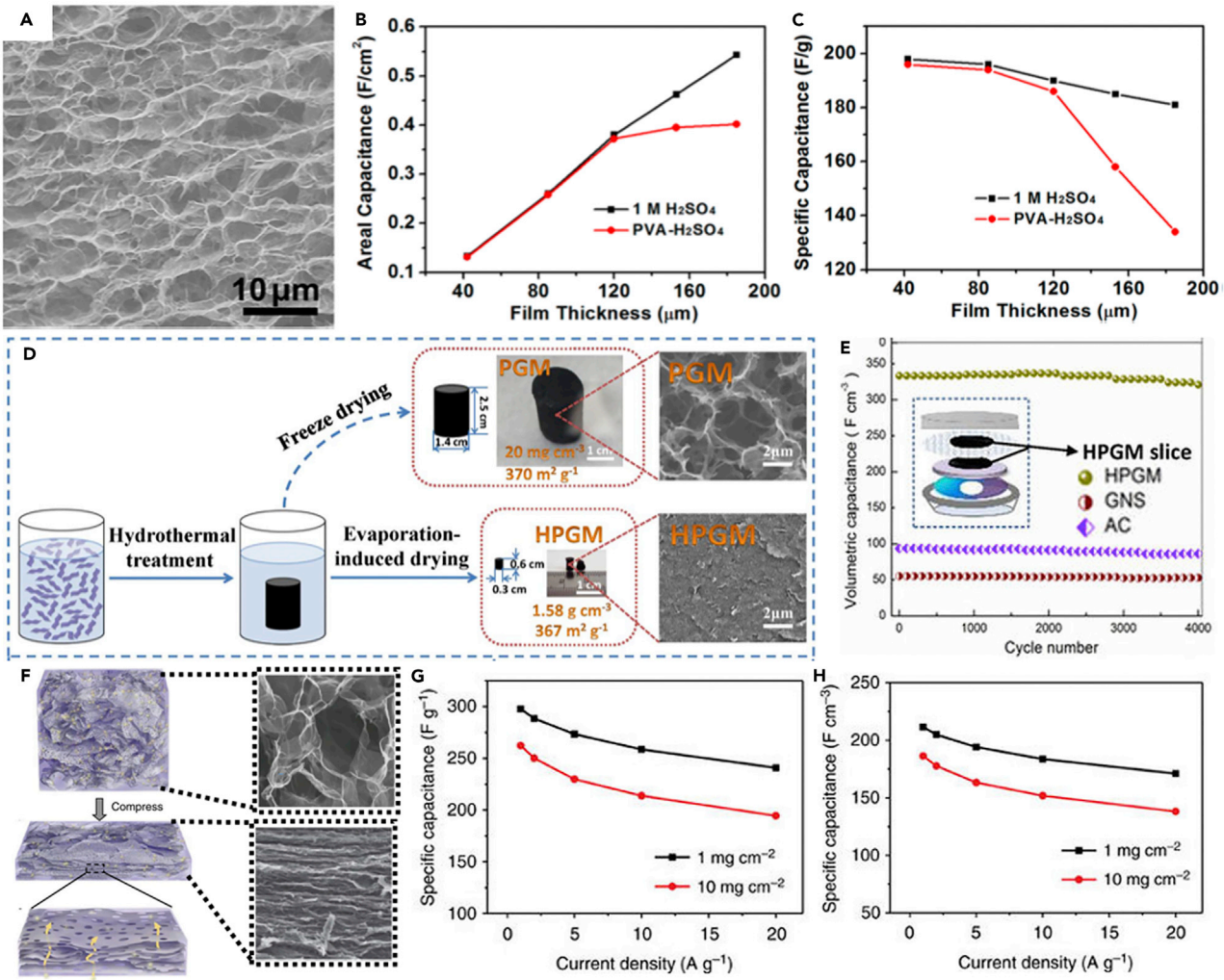

Figure 7. Compressed Graphene Hydrogel/Aerogels for EDLC Electrodes

(A–C) SEM image of the interior microstructure of the graphene hydrogel before pressing (A). Thickness dependence of (B) areal capacitance and (C) mass-specific capacitance of a graphene hydrogel film comparing a liquid (1 M H_2SO_4) and a gel (H_2SO_4-PVA) electrolyte at current density of 1 A/g. Reprinted with permission from Xu et al.[49] Copyright 2013, American Chemical Society.

(D) Schematic of the formation of graphene-based 3D porous macroforms with different drying process and the SEM images of the resultant PGM and HPGM.

(E) Cycle performance of HPGM, GNS (powdered graphene), and AC at a current density of 0.5 A/g (the inset is a diagram of the two-electrode measurement device). Reprinted with permission from Springer Customer Service Center GmbH: Springer Nature, *Scientific Reports*, Tao et al.,[112] Copyright 2013.

(F–H) Schematic illustration of the HGFs as an ideal material for EDLC electrodes (F). Gravimetric (G) and volumetric (H) capacitances of HGF electrodes versus different current densities (with graphene mass loading of 1 and 10 mg/cm^2). Reprinted with permission from Springer Customer Service Center GmbH: Springer Nature, Nature Communications, Xu et al.,[45] Copyright 2014.

neatly packed graphene sheets and without identified opening pores (Figure 7D). This is totally different from spongy porous graphene macroform (PGM) with large pores (formed by commonly used freeze-drying). The HPGM has a low oxygen content of 16 atom % and an acceptable conductivity of ~16 S/m due to the partial reduction and the tight interlinkage of graphene nanosheets. Furthermore, its large surface area (367 m^2/g), porous microstructure (pore volume of 0.16 cm^3/g), and large density (1.58 g/cm^3) led to a high volumetric capacitance of 376 F/cm^3 in aqueous electrolyte (Figure 7E). However, its corresponding areal capacitance was not reported. Xu et al.

designed a compact holey graphene framework (HGF) to achieve a large mass loading of 10 mg/cm^2, leading to high gravimetric (298 F/g) and volumetric (212 F/cm^3) capacitances as well as ultrahigh areal capacitance (2.65 F/cm^2) in organic electrolyte (Figures 7G and 7H).[45] The HGF was synthesized by a one-step hydrothermal reaction with aqueous solution of H_2O_2. Its 3D networks were constructed by graphene self-assembly and its abundant nanoscaled in-plane pores across the entire graphene surface network were created by *in situ* H_2O_2 etching at low temperature. Thus, a large BET surface area of 830 m^2/g was obtained for HGFs, which is significantly larger than that of nonholey graphene frameworks. Furthermore, the as-prepared HGF was hydraulically pressed to form a free-standing compact structure (Figure 7F), resulting in nearly 60-fold increase of packing density (0.71 g/cm^3) without sacrificing surface area (810 m^2/g). The HGF also possesses high conductivity (about 1,000 S/m). Therefore, the compact HGF films meet the critical requirements for an ideal EDLC electrode: (1) its entire surface area is fully accessible even after mechanically compressing due to highly porous monolithic framework of interconnected and interlocked graphene and abundant nanopores in holey graphene sheets; and (2) sufficiently large nanopores in holey graphene sheets can act as shortcuts between different layers of graphene, speeding up ion transport. The similar strategies were further modified by Shi and coworkers to develop 3D hydroxyl-rich graphene hydrogels (HRGHs), which exhibited an ultrahigh areal capacitance of 2.67 F/cm^2 at 1 mA/cm^2 with a large HRGH mass loading of 10 mg/cm^2 and excellent gravimetric and volumetric capacitances (260 F/g and 312 F/cm^3 at 1 A/g).[79] The 3D structure was prepared via an improved hydrothermal process, and the compact structure with packing density of 1.2 g/cm^3 was achieved by mechanically compressing the fully immersed HRGHs under 1-MPa pressure. During hydrothermal reduction, hydroxyl groups on GO sheets were reserved due to introduction of n mol/L H_3PO_4 (n = 0, 0.1, 0.2, and 0.4) as the hydroxyl protecting agent, which improved the wettability of HRGHs to aqueous electrolyte and brought about extra pseudocapacitance. The well-maintained surface areas (998 m^2/g) after pressing and the good conductivity (92 S/m) of the 3D HRGH can explain its excellent performance for EDLCs.

Highly Dense Graphene/Carbon Spacer Frameworks. Other carbon spacers (sphere, tube, fabric) were also employed to tune the spaces between graphene sheets for the well-designed highly dense graphene/spacer electrodes, in which large mass loadings were achieved.[113–118] For example, Zheng and coworkers vacuum-filtrated multiwall carbon nanotube (MWCNT, 10 mg/mL) and rGO (5 mg/mL) directly onto Ni-coated cotton fabrics.[119] Consequently, thick electrodes with nanoscale porosity were successfully fabricated on textiles, and the interfacial contact and adhesion at the metal/carbon interfaces were significantly improved. Furthermore, the composite fabric electrodes were easily scaled up from 0.4 to 23.7 mg/cm^2 through alternative filtration cycles, reaching the highest thickness of ~400 μm and thus achieving an ultrahigh areal capacitance of 6.20 F/cm^2 at a rate of 20 mA/cm^2. Therefore, we can conclude that a suitable spacer between graphene sheets is a critical factor in obtaining a high packing density without losing accessible surface area and thus reaching well-balanced gravimetric, volumetric, and areal capacitances.

Scalable Electrodes Based on Directly Synthesized 3D Graphene

In recent years a new strategy, "direct synthesis of 3D graphene," has been developed to prepare novel graphene materials. It can greatly maintain the properties of individual graphene sheets and simplify the synthetic process. Furthermore, the obtained 3D graphene exhibited high electrical conductivity and structural stability.[120] Although the template chemical vapor deposition method[37,121] and sugar-blowing approach[122] were utilized to prepare 3D graphene, the obtained product

has a small yield and a low density that limit its applications. To solve these issues, Hu and coworkers discovered a series of new reactions for 3D graphene synthesis.[38,54–57] These one-step processes, conducted in a batch-mode ceramic tube reactor, can produce 3D graphene with a high yield. Furthermore, its novel morphology, easily tuned pore structure, and flexible surface modification can be delicately controlled by adjusting reaction temperature (pressure or time) and changing reactants to meet specific requirements. Moreover, moderate reaction conditions (below 600°C), easy operation, and a simple synthetic system constitute a great possibility for its large-scale production and wide application.

Scalable Mesoporous Graphene Electrodes. The 3D honeycomb-like structured graphene (HSG) has been successfully constructed by Hu's discovered reaction between Li_2O particles and CO gas (Figure 8A).[38] The feasibility of this reaction was first demonstrated by thermodynamic calculation, indicating their thermodynamically favorable feature (negative Gibbs free energy change) and energy-economic property (negative enthalpy change). Its honeycomb-like structure (Figures 8B and 8C) was controlled by simultaneously generated Li_2CO_3 nanoparticles, leading to surface area of 151 m^2/g and pore sizes in the range from 115 to 170 nm. Although the 3D HSG with high electrical conductivity and some oxygen-functional groups exhibited a high-power conversion efficiency for dye-sensitized solar cells, its application for supercapacitors was limited by its relatively small surface area. To solve this issue, the reaction between lithium liquid and CO_2 was designed to synthesize 3D cauliflower-fungus-like graphene (CFG, Figure 8D),[54] a mesoporous material with improved surface area of 462 m^2/g and concentrated pore size of 2–70 nm. The simultaneous generation of Li_2CO_3 particles can isolate graphene sheets, control the graphene shape, and prevent graphite formation. The entire surface area of the CFG electrodes in EDLCs could be accessed by electrolyte ions due to facilitated ion transport within a hierarchical porous structure, achieving a large CFG mass loading of 11.16 mg/cm^2 and thus a very high areal capacitance of 1.16 F/cm^2, and good gravimetric and volumetric capacitances (103.6 F/g and 120 F/cm^3) at a rate of 1 A/g (Figures 8E and 8F). Furthermore, these CFG electrodes were operated at relatively high temperature (55°C), showing rectangular cyclic voltammetry curves, good rate performance, and cycling stability.

Scalable Surface Microporous Graphene Electrodes with Meso-/Macrochannels. It is well known that AC used in commercial EDLCs is a microporous material with unsatisfactory electrochemical performance. This happens because of two conflicting roles of micropores in EDLCs, namely, although micropores can enhance charge accumulation to form EDLs, their very small pore sizes inhibit ion transport at a high rate with a large mass loading. This drawback was solved by 3D surface microporous graphene (SMG). Hu and coworkers synthesized the SMG material with a large surface area of 890 m^2/g by reacting Na liquid with CO_2, achieving a gravimetric capacitance of 200 F/g.[55] In this process, CO_2 gas played two important roles (Figure 8G): (1) CO_2 generated graphene sheets by its reaction with Na liquid, and the produced Na_2CO_3 nanoparticles controlled the shape of graphene and prevented graphene aggregation; and (2) CO_2 *in situ* oxidized graphene walls to create surface micropores. The obtained SMG (Figures 8H and 8I) possessed a cabbage-coral-like shape with meso-/macrochannels built by coiled and bent graphene sheets, abundant surface micropores with average deepness of 0.54 nm distributed on 2.2-nm-thick graphene sheets, and oxygen modification (4.88%) with existence of C–O and C=O groups. The channels with a range from 200 nm to 1 μm can buffer electrolyte as a reservoir. The buffered electrolyte

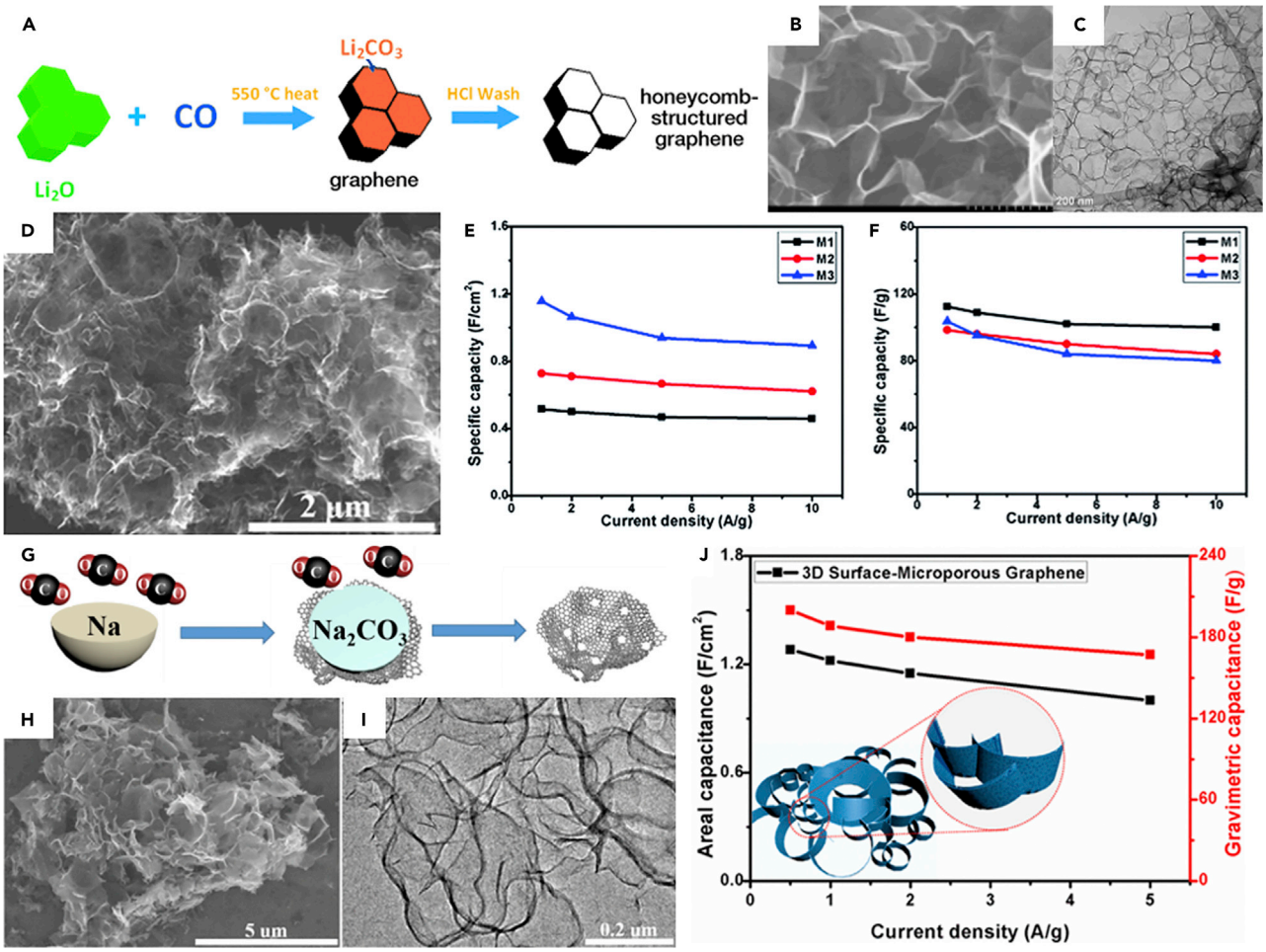

Figure 8. Directly Synthesized 3D Graphene for EDLC Electrodes

(A) Schematic of synthesis of honeycomb-structured graphene.

(B and C) SEM image (B) and transmission electron microscopy (TEM) image (C) of HSG. Adapted with permission from Wang et al.[38] Copyright 2013, Wiley-VCH Verlag GmbH & Co. KGaA, Weinheim.

(D) Field-emission SEM image of CFG.

(E and F) Areal capacitance (E) and gravimetric capacitance (F) of 3D graphene-based supercapacitors with different graphene-mass loadings (M1, 4.58 g/cm^2; M2, 7.40 g/cm^2; M3, 11.16 g/cm^2) versus current density at room temperature. Reproduced from Chang et al.,[54] with permission from the Royal Society of Chemistry.

(G) Illustration of reaction: SMG formation with Na and CO_2 reaction, and simultaneous pore-creation-reaction between graphene and CO_2.

(H and I) SEM image (H) and TEM image (I) of SMG.

(J) Areal and gravimetric capacitance of SMG (inset is illustration of SMG structure). Reprinted with permission from Chang et al.[55] Copyright 2017, American Chemical Society.

can directly touch the graphene walls and transfer to the surface micropores of SMG electrodes with a negligible transport distance to form efficient EDLs at a high rate. Therefore, the SMG electrodes were scaled up with a large mass loading, leading to a very high areal capacitance of 1.28 F/cm^2 (Figure 8J) and excellent rate capability (83.5% from 0.5 to 10 A/g) as well as high cycling stability (86.2% retention after 5,000 cycles). The reaction between K and CO_2 was also demonstrated to produce 3D surface microporous graphene with excellent performance for supercapacitors.[56] From the above discussion, one can see that CFG and SMG can meet the following two requirements for an ideal electrode material: (1) large accessible surface area for electrolyte to form EDLs and (2) highly

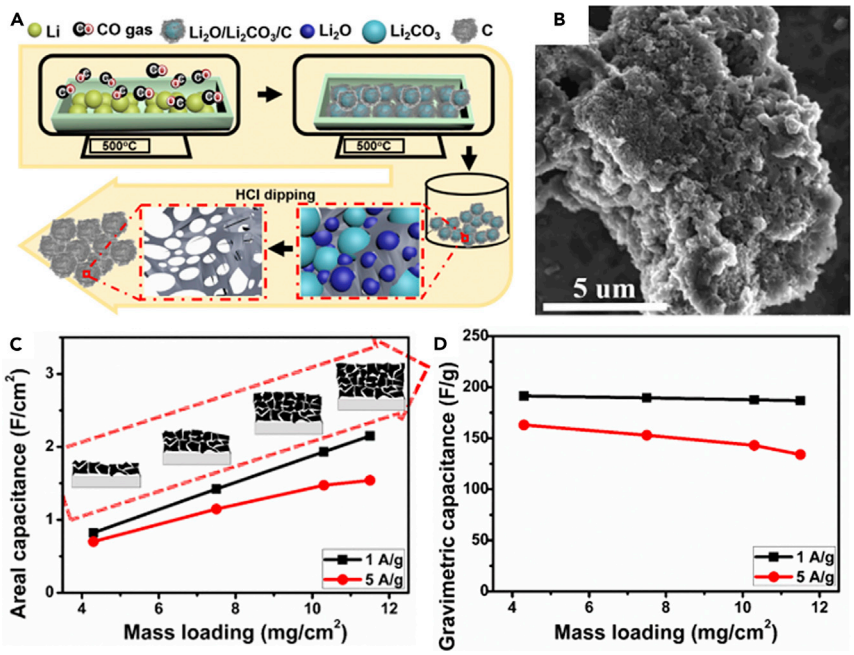

Figure 9. 3D Graphene with High Packing Density for EDLC Electrodes

(A) Schematic process for DMPC synthesis.

(B–D) SEM image of DMPC (B). Mass-loading effect of DMPC on (C) areal capacitance and (D) gravimetric capacitance (1 and 5 A/g current densities). Reprinted with permission from Chang et al.[57] Copyright 2018, American Chemical Society.

interconnected carbon frameworks and hierarchical porous networks for continuous and rapid ion transport.[123]

Scalable Porous Graphene Electrodes with High Packing Density. In addition to accessible surface areas and continuous ion/electron transport routes, packing density is a key parameter for an electrode material. A dense electrode would be of vital importance for well-balanced capacitance in gravimetric, volumetric, and areal scales, especially in a packaged EDLC device. However, it is a challenge to synthesize highly dense porous carbon (DMPC). Very recently, a new chemistry between Li liquid and CO gas was discovered for directly synthesizing DMPC.[57] A high packing density of 1.94 g/cm^3 was achieved in such a mesoporous carbon material with a large surface area of 857 m^2/g. This unique feature originates from its synthesis process (Figure 9A). The reaction between Li liquid and CO gas produced DMPC/Li_2O/Li_2CO_3 composites. The *in situ*-formed templates (Li_2O/Li_2CO_3) well controlled the size and distribution of 40-nm mesopores, while the interspaces of stacked graphene layers created large amounts of 6-nm mesopores. After removing Li_2O and Li_2CO_3 by HCl, one can see volcanic-scoria-like carbon with large primary particle size larger than 5 μm (Figure 9B). These large primary particles contribute to its high packing density due to the great decrease in the total interparticle spaces. Such a novel DMPC exhibited excellent performance as electrodes in a symmetrical EDLC, achieving large gravimetric capacitance of 205.2 F/g and high volumetric capacitance of 220.5 F/cm^3 at a rate of 0.5 A/g. Furthermore, its areal capacitance showed a linear relationship with mass loading and reached the ultrahigh value of 2.15 F/cm^2 at a large mass loading of 11.5 mg/cm^2 (Figure 9C). This excellent performance in areal scale was attributed to the negligible effect of mass loading on its gravimetric

capacitance (Figure 9D). Therefore, DMPC electrodes solved the trade-off issue for capacitance in three scales (gravimetric, volumetric, and areal).

Conclusion and Perspective

From the viewpoint of graphene design and synthesis, we evaluated the recent progress in graphene electrodes for supercapacitors with emphasis on commercial requirements. It was demonstrated how important and challengeable it is for a supercapacitor to obtain high values for all three types of capacitances (gravimetric, volumetric, and areal capacitances) at commercial-level mass loading of 10 mg/cm^2 or thickness of about 200 μm.

The ideal electrode materials for highly efficient EDLCs must possess large accessible surface area, continuous and fast electron/ion transport pathways, and large packing density. The two types of strategies were discussed for design and synthesis of scalable and ideal graphene electrodes: the reconstruction of 2D graphene (to 0D, 1D, 2D, and 3D macroscale architectures) and the direct synthesis of 3D graphene. Several breakthroughs have been obtained with novel graphene electrode materials for EDLCs in recent years (Table 1). Twelve types of graphene electrodes have achieved ultrahigh areal capacitances above 1.00 F/cm^2 with a large mass loading at a high rate of 1 A/g, and half of them are even larger than 2.00 F/cm^2 with very large mass loading of 10 mg/cm^2 or above (Figure 10). Furthermore, among them the two largest areal capacitances were achieved by two types of graphene-based electrodes, namely, 6.20 F/cm^2 at 20 mA/cm^2 with the MWCNTs/rGO composite electrode and 7.40 F/cm^2 at 1 mA/cm^2 with the electrode of the HAGFFs. Without doubt, the novel synthetic approaches of graphene materials, which are based on new chemistry and new technologies,[54,55,57,124–126] will play a critical role in the development of commercialized graphene-based EDLCs with excellent performance at low cost.

So far, however, the best capacitance of graphene-based electrodes is still far below its theoretical value of 526 F/g. It would be a challenge to achieve the theoretical value for graphene-based EDLCs. This may stimulate the following future research: (1) to increase the accessible surface area of synthesized graphene material close to its theoretical surface area (2,630 m^2/g), (2) to design pore structures that can balance the electrolyte-ion transfer requirement and the high packing density, and (3) to tune the surface charge for boosting capacitance and expanding the operating voltage. On the other hand, the newly discovered features of graphene (such as unconventional superconductivity in magic-angle graphene superlattices[127,128]) present tremendous advantages for the design of new-concept supercapacitors, such as flexible micro-supercapacitors, fiber supercapacitors, and Li/Na-ion capacitors.[129–131] This may open a new era for supercapacitors.

Besides the important research progress, graphene-based EDLCs have emerged on the market, and are obtaining strong technical and financial support from many companies and investment agencies.[132–134] For example, ZapGo, a UK company with a grant from European Union's Horizon 2020 research and innovation program, is engaged to develop ultra-fast-charge graphene-enhanced supercapacitors. Skeleton Technologies (the largest supercapacitor manufacturer in Europe) manufactures the curved graphene for SkelCap cells, achieving a production capacity of 4 million cells a year. Ningbo CSR New Energy Technology in China developed two new types of supercapacitors: (1) 3 V/12,000 farads with electrodes of composite of graphene and AC, and (2) 2.8 V/30,000 farads in graphene nanohybrid. These new supercapacitors can make a trolleybus travel 10 km after a charge of 1 min.

Table 1. Gravimetric, Areal, and Volumetric Capacitances of Graphene-Based EDLCs

Electrode Materials	S_{BET} (m^2/g)	Conductivity (S/cm)	Electrolyte	V (V)	Mass Loading (mg/cm^2)	i (A/g)[a] or i (mA/cm^2)[b] or v (V/s)[c]	$C_{gravimetric}$ (F/g)	C_{areal} (mF/cm^2)	C_{vol} (F/cm^3)	Ref.
Exfoliation of graphitic oxide	925		1 M H_2SO_4	0–1	3	0.1[c]	117			Vivekchand et al.,[31] 2008
						1[c]	100			
Chemically modified graphene	705	2	5.5 M KOH	0–1	3.7	10[b]	135			Stoller et al.,[33] 2008
			$TEABF_4$/AN	0-2.5			99			
Activated microwave-exfoliated GO	2,400		(BMIM BF_4)/AN	0–3.5		1.4[a]	165		60	Zhu et al.,[35] 2011
Activated GO film	2,400	58.8	$TEABF_4$/AN	0–2.5		10[a]	120			Zhang et al.,[43] 2012
Sulfur and nitrogen codoped mesoporous graphene	1,500		6 M KOH	0–0.9		1[a]	116			Ma et al.,[47] 2018
Self-assembled graphene hydrogel		5×10^3	5 M KOH	0–1		0.01[c]	175			Xu et al.,[36] 2010
Nitrogen-doped carbon dots/3D graphene	56		6 M KOH	−0.9 to 0.1	2–2.5	0.5[a]	338*	0.604*		Yuan et al.,[50] 2019
3D functionalized graphene	362		6 M KOH	0–1	1.5–3	0.5[a]	326			Tian et al.,[51] 2015
3D nitrogen, boron-codoped graphene	249		PVA/H_2SO_4 gel	0–1		0.005[c]	62			Wu et al.,[52] 2012
Laser-scribed graphene	1,520	17.38	1 M H_3SO_4	0–1		1[a]		4.04		El-Kady et al.,[64] 2012
			PVA/H_3PO_4			1[a]		3.67		
						1,000[a]		1.82		
3D carbon foam with multiscale pores	2,905	3	3 M KOH	0 to −0.8	2.5	1[a]	374.7*			Zhang et al.,[68] 2017
3D graphene gel	614.9	1.033	1 M H_2SO_4	0–1		1[b]		33.8		Maiti et al.,[76] 2014
Holey graphene papers	217	20.3	1 M H_2SO_4	0–1		1[a]	209		234	Xu et al.,[87] 2015
rGO foams			1 M H_2SO_4	0–0.8		0.5[a]	110			Niu et al.,[81] 2012
N-doped graphene framework	280		1 M $LiClO_4$	0–0.8		1[a]	484*			Zhaoet al.,[82] 2012
Crumpled graphene balls (CGBs)	567		5 M KOH	0–0.8	2.5	0.1[a]	150			Luo et al.,[89] 2013
						2[a]	118		58	
					20	0.1[a]	150	2,700[§]		
						1[a]	105	2,010[§]		
						2[a]	73	1,260[§]		
Activated microwave-expanded GO	3,290		[EMIM][TFSI]/AN	0–3.5	1.3	1.1[a]	174		100	Kim et al.,[90] 2013
					10.4		129		58	
CGBs (0.7 μm)			5 M KOH	0–1	2.5	1[a]	156			Jo et al.,[91] 2016

(*Continued on next page*)

Table 1. *Continued*

Electrode Materials	S_{BET} (m^2/g)	Conductivity (S/cm)	Electrolyte	*V* (V)	Mass Loading (mg/cm^2)	*i* (A/g)[a] or *i* (mA/cm^2)[b] or *v* (V/s)[c]	$C_{gravimetric}$ (F/g)	C_{areal} (mF/cm^2)	C_{vol} (F/cm^3)	Ref.
Porous carbon nanotube networks Decorated CGBs	260		6 M KOH	0–1	0.13	0.325[a]	202	230	9.59	Mao et al.,[92] 2014
					1.15		147			
Hierarchical porous graphene	695		PVA/KOH	0–1	0.83	1[b]		220		Li et al.,[93] 2017
Graphene fibers	325	106	PVA/H_2SO_4	−0.2 to 0.8		36[b]			45*	Fan et al.,[98] 2016
Graphene-based coaxial fiber			PVA/H_2SO_4	0–0.8	2.25	0.01[c]	182		205	Zhao et al.,[100] 2015
Graphene fiber			PVA/H_2SO_4	0–0.8		0.05[c]		0.443	0.526	Yu et al.,[101] 2017
3D mesoporous plasma-reduced GO web	642	87	1 M H_2SO_4	0–0.8		0.2[a]	253.8*			Lee et al.,[102] 2017
			PVA/H_2SO_4				54.9			
Surface-porous graphene fibers	839	567	PVA/H_2SO_4	0–1		0.0397[b]		228		Cai et al.,[104] 2015
Porous graphene ribbons	697	120	H_3PO_4/PVA	0–0.8		0.1[a]	208.7	78.3		Huang et al.,[105] 2015
Hydrothermally activated graphene fiber fabrics	245	0.04	1 M H_2SO_4	0–0.8	150 μm film	0.1[a]	244	1,060		Li et al.,[106] 2017
						1[a]	233	1,012[#]		
					5 × 200 μm film	1[b]		7,398		
						1[a]		4,000[#]		
Self-stacked, solvated graphene (SSG)		1,860 Ω/sq	1 M H_2SO_4	0–1	0.045	1.08[a]	215			Yang et al.,[110] 2011
Electrolyte-mediated chemically converted graphene			1 M H_2SO_4	0–1	1	0.1[a]	191.7		255.3	Yang et al.,[65] 2013
					10	1[a]		1,570[§]		
			EMIMBF$_4$	0–3.5	1	0.1[a]	209		261.3	
Graphene hydrogel	414	1.92	H_2SO_4/PVA	0–1	2	1[a]	186	372		Xu et al.,[49] 2013
3D graphene aerogels	504	2.73	0.5 M H_2SO_4	0–1		1[a]	325			Jung et al.,[111] 2015
High-density porous graphene macroform	720	1.15	6 M KOH	0–1		0.1[a]	238		376	Tao et al.,[112] 2013
Holey graphene framework	830	10	6 M KOH	0–1	1	1[a]	310			Xu et al.,[45] 2014
			EMIMBF$_4$/AN	0–3.5			298		212	
					10		262	2,650[§]		
Hydroxyl-rich graphene hydrogels	998	0.92	1 M H_2SO_4	0–1	1	1[a]	260		312	Ma et al. [79] 2018
					10	1[b]		2,675		
						1[a]		2,400[#]		
3D hierarchical porous graphene	1,810	10	6 M KOH	0–1	1	0.5[a]	305			Li et al.,[113] 2013

(*Continued on next page*)

Table 1. *Continued*

Electrode Materials	S_{BET} (m^2/g)	Conductivity (S/cm)	Electrolyte	*V* (V)	Mass Loading (mg/cm^2)	*i* (A/g)[a] or *i* (mA/cm^2)[b] or *v* (V/s)[c]	$C_{gravimetric}$ (F/g)	C_{areal} (mF/cm^2)	C_{vol} (F/cm^3)	Ref.
Carbon nanotube bridged graphene 3D building blocks	652	394	$EMIBF_4$	0–4	0.6–1	0.5[a]	199		211	Pham et al.,[114] 2015
3D few-layer graphene and carbon nanotube foam	743		6 M KOH	0–1		1.78[b]	285			Wang et al.,[116] 2013
3D architecture of graphene aerogels/porous carbon fabrics	322		PVA/KOH	0–1	5	0.1[a]	391			Song et al.,[117] 2015
Partially reduced GO/carbon nanotube composites	240		6M KOH	0–1.2	12	1[a]			255	Diez et al.,[118] 2018
MWCNT/rGO ten-bilayer hybrid	166		5 M LiCl	0–1	23.7	20[b]	250	6,200	107	Yang et al.,[119] 2017
Hollow porous graphene balls	1,871		6 M KOH	0–1	5	0.05[a]	321		114	He et al.,[120] 2014
Nitrogen-doped mesoporous carbon	1,580	360	2 M Li_2SO_4	0–1.6	0.5	1[a]	790		490	Lin et al.,[121] 2015
					6		710			
3D strutted graphene	1,005	200	1 M H_2SO_4	0–1	1	1[a]	250			Wang et al.,[122] 2013
						100[a]	130			
3D cauliflower-fungus-like graphene	462		2 M KOH	0–1	4.58	1[a]	112.4	520	120	Chang et al.,[54] 2015
					11.16		103.6	1,160		
Surface microporous graphene	890		2 M KOH	0–1	2.8	0.5[a]	200	560		Chang et al.,[55] 2017
					6.4		199.7	1,280		
						1[a]	190.2	1,220[§]		
Meso-/macroporous frameworks of surface microporous graphene	1,031		2 M KOH	0–1	2.6	2[a]	160.4			Chang et al.,[56] 2017
					6.3	1[a]	167.8	1,057[§]		
						2[a]	159.2			
3D potassium-ion pre-intercalated graphene	990		2 M KOH	0–1	3	1[a]	183.8	550		Chang et al.,[23] 2018
					8		187	1,500		
Na-embedded carbon nanowalls	555	5.24	2 M KOH	0–1	4	1[a]	143.2	570	143.2	Chang et al.,[73] 2017
					8		143	1,140	143	
Highly dense mesoporous carbon	857		2 M KOH	0–1	4.3	0.5[a]	205.2	823	220.5	Chang et al.,[57] 2018
					11.5	1[a]	186.8	2,150		

The default test cell is a two-electrode configuration. The data from three-electrode configuration are labeled with an asterisk (*). S_{BET}, BET surface area; *V*, potential; *i*, current density; *v*, scan rate (a, b, and c indicate date from current per electrode mass, current per electrode area and scan rate); $C_{gravimetric}$, gravimetric capacitance; C_{areal}, areal capacitance ([§] and [#] indicate values from calculation and estimation based on the data in the respective references); C_{vol}, volumetric capacitance.

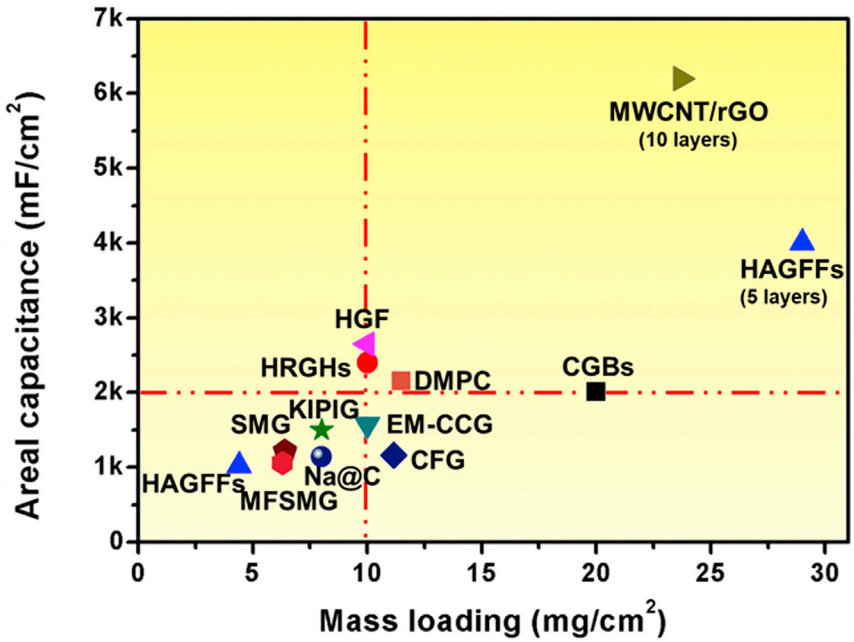

Figure 10. Breakthrough of Graphene Electrodes for EDLCs

Reported areal capacitance of graphene electrodes at a high-level mass loading for EDLCs (current density, 1 A/g): potassium-ion pre-intercalated graphene (KIPIG),[23] holey graphene framework (HGF),[45] crumpled graphene balls (CGBs),[89] cauliflower-fungus-like graphene (CFG),[54] surface microporous graphene (SMG),[55] meso-/macroporous frameworks of surface microporous graphene (MFSMG),[56] highly dense mesoporous carbon (DMPC),[57] electrolyte-mediated chemically converted graphene (EM-CCG),[65] Na-embedded carbon nanowalls (Na@C),[73] hydroxyl-rich graphene hydrogels (HRGHs),[79] hydrothermally activated graphene fiber fabrics (HAGFFs),[106] and multiwall carbon nanotube/reduced GO hybrids (MWCNT/rGO).[119]

Nevertheless, great R & D efforts are still needed to decrease the production cost of recently developed superior graphene materials before they can be applied to commercial energy-storage devices on a large scale.

ACKNOWLEDGMENTS

This work was supported by US National Science Foundation (CMMI1661699).

AUTHOR CONTRIBUTIONS

Y.H.H. and L.C. made contributions to the manuscript preparation. Y.H.H. wrote the manuscript.

REFERENCES

1. Mai, L., Tian, X., Xu, X., Chang, L., and Xu, L. (2014). Nanowire electrodes for electrochemical energy storage devices. Chem. Rev. *114*, 11828–11862.

2. Wang, H., Zhu, C., Chao, D., Yan, Q., and Fan, H.J. (2017). Nonaqueous hybrid lithium-ion and sodium-ion capacitors. Adv. Mater. *29*, 1702093.

3. Ye, M., Zhang, Z., Zhao, Y., and Qu, L. (2018). Graphene platforms for smart energy generation and storage. Joule *2*, P235–P268.

4. Ratajczak, P., Suss, M.E., Kaasik, F., and Beguin, F. (2019). Carbon electrodes for capacitive technologies. Energy Storage Mater. *16*, 126–145.

5. Zhang, L.L., Zhou, R., and Zhao, X.S. (2010). Graphene-based materials as supercapacitor electrodes. J. Mater. Chem. *20*, 5983–5992.

6. Zheng, S., Tang, X., Wu, Z.S., Tan, Y.Z., Wang, S., Sun, C., Cheng, H.M., and Bao, X. (2017). Arbitrary-shaped graphene-based planar sandwich supercapacitors on one substrate with enhanced flexibility and integration. ACS Nano *11*, 2171–2179.

7. Chang, L., and Hu, Y.H. (2018). 2.21 supercapacitors. Compr. Energy Syst. *2*, 663–695.

8. Winter, M., and Brodd, R.J. (2004). What are batteries, fuel cells, and supercapacitors? Chem. Rev. *104*, 4245–4270.

9. Liu, J., Wang, J., Xu, C., Jiang, H., Li, C., Zhang, L., Lin, J., and Shen, Z.X. (2018). Advanced energy storage devices: basic

principles, analytical methods, and rational materials design. Adv. Sci. *3*, 1700322.

10. Simon, P., Gogotsi, Y., and Dunn, B. (2014). Where do batteries end and supercapacitors begin? Science *343*, 1210–1211.

11. Simon, P., and Gogotsi, Y. (2008). Materials for electrochemical capacitors. Nat. Mater. *7*, 845–854.

12. Hwang, J.Y., Li, M., El-Kady, M.F., and Kaner, R.B. (2017). Next-generation activated carbon supercapacitors: a simple step in electrode processing leads to remarkable gains in energy density. Adv. Funct. Mater. *27*, 1605745.

13. Xu, Y., Chang, L., and Hu, Y.H. (2017). KOH-assisted microwave post-treatment of activated carbon for efficient symmetrical double-layer capacitors. Int. J. Energy Res. *41*, 728–735.

14. Banda, H., Perie, S., Daffos, B., Dubois, L., Crosnier, O., Simon, P., Taberna, P.L., and Duclairoir, F. (2019). Investigation of ion transport in chemically tuned pillared graphene materials through electrochemical impedance analysis. Electrochim. Acta *296*, 882–890.

15. Yu, Z., Tetard, L., Zhai, L., and Thomas, J. (2015). Supercapacitor electrode materials: nanostructures from 0 to 3 dimensions. Energy Environ. Sci. *8*, 702–730.

16. Zheng, S., Li, Z., Wu, Z.S., Dong, Y., Zhou, F., Wang, S., Fu, Q., Sun, C., Guo, L., and Bao, X. (2017). High packing density unidirectional arrays of vertically aligned graphene with enhanced areal capacitance for high-power micro-supercapacitors. ACS Nano *11*, 4009–4016.

17. Wang, G., Zhang, L., and Zhang, J. (2012). A review of electrode materials for electrochemical supercapacitors. Chem. Soc. Rev. *41*, 797–828.

18. Peng, L., Fang, Z., Zhu, Y., Yan, C., and Yu, G. (2018). Holey 2D nanomaterials for electrochemical energy storage. Adv. Energy Mater. *8*, 1702179.

19. Novoselov, K.S., Geim, A.K., Morozov, S.V., Jiang, D., Zhang, Y., Dubonos, S.V., Grigorieva, I.V., and Firsov, A.A. (2004). Electric field effect in atomically thin carbon films. Science *306*, 666–669.

20. Morozov, S.V., Novoselov, K.S., Katsnelson, M.I., Schedin, F., Elias, D.C., Jaszczak, J.A., and Geim, A.K. (2008). Giant intrinsic carrier mobilities in graphene and its bilayer. Phys. Rev. Lett. *100*, 016602.

21. Balandin, A.A., Ghosh, S., Bao, W.Z., Calizo, I., Teweldebrhan, D., Miao, F., and Lau, C.N. (2008). Superior thermal conductivity of single-layer graphene. Nano Lett. *8*, 902–907.

22. Nair, R.R., Blake, P., Grigorenko, A.N., Novoselov, K.S., Booth, T.J., Stauber, T., Peres, N.M.R., and Geim, A.K. (2008). Fine structure constant defines visual transparency of graphene. Science *320*, 1308.

23. Chang, L., Stacchiola, D.J., and Hu, Y.H. (2018). Design and synthesis of 3D potassium-ion pre-intercalated graphene for supercapacitors. Ind. Eng. Chem. Res. *57*, 3610–3616.

24. El-Kady, M.F., Shao, Y., and Kaner, R.B. (2016). Graphene for batteries, supercapacitors and beyond. Nat. Rev. Mater. *1*, 16033.

25. Lim, J., Lee, G.Y., Lee, H.J., Cha, S.K., Choi, D.S., Koo, S.H., Lee, W.J., and Kim, S.O. (2019). Open porous graphene nanoribbon hydrogel via additive-free interfacial self-assembly: fast mass transport electrodes for high-performance biosensing and energy storage. Energy Storage Mater. *16*, 251–258.

26. Song, Y., Liu, T., Qian, F., Zhu, C., Yao, B., Duoss, E., Spadaccini, C., Worsley, M., and Li, Y. (2018). Three-dimensional carbon architectures for electrochemical capacitors. J. Colloid Interface Sci. *509*, 529–545.

27. Raccichini, R., Varzi, A., Passerini, S., and Scrosati, B. (2015). The role of graphene for electrochemical energy storage. Nat. Mater. *14*, 271–279.

28. Yang, M., and Zhou, Z. (2017). Recent breakthroughs in supercapacitors boosts by nitrogen-rich porous carbon materials. Adv. Sci. *4*, 1600408.

29. Zhang, C., and Nicolosi, V. (2019). Graphene and MXene-based transparent conductive electrodes and supercapacitors. Energy Storage Mater. *16*, 102–125.

30. Lv, T., Liu, M., Zhu, D., Gan, L., and Chen, T. (2018). Nanocarbon-based materials for flexible all-solid-state supercapacitors. Adv. Mater. *30*, 1705489.

31. Vivekchand, S.R.C., Rout, C.S., Subrahmanyam, K.S., Govindaraj, A., and Rao, C.N.R. (2008). Graphene-based electrochemical supercapacitors. J. Chem. Sci. *120*, 9–13.

32. Subrahmanyam, K.S., Vivekchand, S.R.C., Govindaraj, A., and Rao, C.N.R. (2008). A study of graphenes prepared by different methods: characterization, properties and solubilization. J. Mater. Chem. *18*, 1517–1523.

33. Stoller, M.D., Park, S., Zhu, Y., An, J., and Ruoff, R.S. (2008). Graphene-based ultracapacitors. Nano Lett. *8*, 3498–3502.

34. Xia, J., Chen, F., Li, J., and Tao, N. (2009). Measurement of the quantum capacitance of graphene. Nat. Nanotechnol. *4*, 505–509.

35. Zhu, Y., Murali, S., Stoller, M.D., Ganesh, K.J., Cai, W., Ferreira, P.J., Pirkle, A., Wallace, R.M., Cychosz, K.A., Thommes, M., et al. (2011). Carbon-based supercapacitors produced by activation of graphene. Science *332*, 1537–1541.

36. Xu, Y., Sheng, K., Li, C., and Shi, G. (2010). Self-assembled graphene hydrogel via a one-step hydrothermal process. ACS Nano *4*, 4324–4330.

37. Chen, Z., Ren, W., Gao, L., Liu, B., Pei, S., and Cheng, H.M. (2011). Three-dimensional flexible and conductive interconnected graphene networks grown by chemical vapour deposition. Nat. Mater. *10*, 424–428.

38. Wang, H., Sun, K., Tao, F., Stacchiola, D.J., and Hu, Y.H. (2013). 3D honeycomb-like structured graphene and its high efficiency as a counter-electrode catalyst for dye-sensitized solar cells. Angew. Chem. Int. Ed. *52*, 9210–9214.

39. Ma, H., Kong, D., Xu, Y., Xie, X., Tao, Y., Xiao, Z., Lv, W., Jang, H.D., Huang, J., and Yang, Q.H. (2017). Disassembly-reassembly approach to RuO_2/graphene composites for ultrahigh volumetric capacitance supercapacitor. Small *13*, 1701026.

40. Bonaccorso, F., Colombo, L., Yu, G., Stoller, M., Tozzini, V., Ferrari, A.C., Ruoff, R.S., and Pellegrini, V. (2015). Graphene, related two dimensional crystals, and hybrid systems for energy conversion and storage. Science *347*, 1246501.

41. Kuila, T., Bose, S., Mishra, A.K., Khanra, P., Kim, N.H., and Lee, J.H. (2012). Chemical functionalization of graphene and its applications. Prog. Mater. Sci. *57*, 1061–1105.

42. Singh, V., Joung, D., Zhai, L., Das, S., Khondaker, S.I., and Seal, S. (2011). Graphene based materials: past, present and future. Prog. Mater. Sci. *56*, 1178–1271.

43. Zhang, L.L., Zhao, X., Stoller, M.D., Zhu, Y., Ji, H., Murali, S., Wu, Y., Perales, S., Clevenger, B., and Ruoff, R.S. (2012). Highly conductive and porous activated reduced graphene oxide films for high-power supercapacitors. Nano Lett. *12*, 1806–1812.

44. Fan, X., Yu, C., Yang, J., Ling, Z., Hu, C., Zhang, M., and Qiu, J. (2015). A layered-nanospace-confinement strategy for the synthesis of two-dimensional porous carbon nanosheets for high-rate performance supercapacitors. Adv. Energy Mater. *5*, 1401761.

45. Xu, Y., Lin, Z., Zhong, X., Huang, X., Weiss, N.O., Huang, Y., and Duan, X. (2014). Holey graphene frameworks for highly efficient capacitive energy storage. Nat. Commun. *5*, 4554.

46. Yang, T., Lin, H., Zheng, X., Loh, K.P., and Jia, B. (2017). Tailoring pores in graphene-based materials: from generation to application. J. Mater. Chem. A *5*, 16537–16558.

47. Ma, X., and Gao, D. (2018). High capacitive storage performance of sulfur and nitrogen codoped mesoporous graphene. Chem. Sus. Chem. *11*, 1048–1055.

48. Biener, J., Stadermann, M., Suss, M., Worsley, M.A., Biener, M.M., Rose, K.A., and Baumann, T.F. (2011). Advanced carbon aerogels for energy applications. Energy Environ. Sci. *4*, 656–667.

49. Xu, Y., Lin, Z., Huang, X., Liu, Y., Huang, Y., and Duan, X. (2013). Flexible solid-state supercapacitors based on three-dimensional graphene hydrogel films. ACS Nano *7*, 4042–4049.

50. Yuan, G., Zhao, X., Liang, Y., Peng, L., Dong, H., Xiao, Y., Hu, C., Hu, H., Liu, Y., and Zheng, M. (2019). Small nitrogen-doped carbon dots as efficient nanoenhancer for boosting the electrochemical performance of three-dimensional graphene. J. Colloid Interface Sci. *536*, 628–637.

51. Tian, W., Gao, Q., Tan, Y., Zhang, Y., Xu, J., Li, Z., Yang, K., Zhu, L., and Liu, Z. (2015). Three-dimensional functionalized graphenes with

systematical control over the interconnected pores and surface functional groups for high energy performance. Carbon *85*, 351–362.

52. Wu, Z.S., Winter, A., Chen, L., Sun, Y., Tuichanim, A., Feng, X., and Mullen, K. (2012). Three-dimensional nitrogen and boron co-doped graphene for high-performance all-solid-state supercapacitors. Adv. Mater. *24*, 5130–5135.

53. Wang, T., Wang, L.X., Wu, D.L., Xia, W., and Jia, D.Z. (2015). Interaction between nitrogen and sulfur in co-doped graphene and synergetic effect in supercapacitor. Sci. Rep. *5*, 9591.

54. Chang, L., Wei, W., Sun, K., and Hu, Y.H. (2015). 3D flower-structured graphene from CO_2 for supercapacitors with ultrahigh areal capacitance at high current density. J. Mater. Chem. A *3*, 10183–10187.

55. Chang, L., Stacchiola, D.J., and Hu, Y.H. (2017). An ideal electrode material, 3D surface-microporous graphene for supercapacitors with ultrahigh areal capacitance. ACS Appl. Mater. Interfaces *9*, 24655–24661.

56. Chang, L., Stacchiola, D.J., and Hu, Y.H. (2017). Direct conversion of CO_2 to meso/macro-porous frameworks of surface-microporous graphene for efficient asymmetrical supercapacitors. J. Mater. Chem. A *5*, 23252–23258.

57. Chang, L., Sun, K., and Hu, Y.H. (2018). New chemistry for new material: highly dense mesoporous carbon electrode for supercapacitors with high areal capacitance. ACS Appl. Mater. Interfaces *10*, 33162–33169.

58. Pak, A.J., and Hwang, G.S. (2016). Molecular insights into the complex relationship between capacitance and pore morphology in nanoporous carbon-based supercapacitors. ACS Appl. Mater. Interfaces *8*, 34659–34667.

59. Paek, E., Pak, A.J., and Hwang, G.S. (2013). A computational study of the interfacial structure and capacitance of graphene in [EMIM][PF_6] ionic liquid. J. Electrochem. Soc. *160*, A1–A10.

60. Paek, E., Pak, A.J., Kweon, K.E., and Hwang, G.S. (2013). On the origin of the enhanced supercapacitor performance of nitrogen-doped graphene. J. Phys. Chem. C *117*, 5610–5616.

61. Pak, A.J., and Hwang, G.S. (2016). Charging rate dependence of ion migration and stagnation in ionic-liquid-filled carbon nanopores. J. Phys. Chem. C *120*, 24560–24567.

62. Stoller, M.D., and Ruoff, R.S. (2010). Best practice methods for determining an electrode material's performance for ultracapacitors. Energy Environ. Sci. *3*, 1294–1301.

63. Balducci, A., Belanger, D., Brousse, T., Long, J.W., and Sugimoto, W. (2017). A guideline for reporting performance metrics with electrochemical capacitors: from electrode materials to full devices. J. Electrochem. Soc. *164*, A1487–A1488.

64. El-Kady, M.F., Strong, V., Dubin, S., and Kaner, R.B. (2012). Laser scribing of high-performance and flexible graphene-based electrochemical capacitors. Science *335*, 1326–1330.

65. Yang, X., Cheng, C., Wang, Y., Qiu, L., and Li, D. (2013). Liquid-mediated dense integration of graphene materials for compact capacitive energy storage. Science *341*, 534–537.

66. Yu, M., Lin, D., Feng, H., Zeng, Y., Tong, Y., and Lu, X. (2017). Boosting the energy density of carbon-based aqueous supercapacitors by optimizing the surface charge. Angew. Chem. Int. Ed. *16*, 5454–5459.

67. Sun, H., Mei, L., Liang, J., Zhao, Z., Lee, C., Fei, H., Ding, M., Lan, J., Li, M., Wang, C., et al. (2017). Three-dimensional holey-graphene/niobia composite architectures for ultrahigh-rate energy storage. Science *356*, 599–604.

68. Zhang, F., Liu, T., Li, M., Yu, M., Luo, Y., Tong, Y., and Li, Y. (2017). Multiscale pore network boosts capacitance of carbon electrodes for ultrafast charging. Nano Lett. *17*, 3097–3104.

69. Wang, Z., Han, Y., Zeng, Y., Qie, Y., Wang, Y., Zheng, D., Lu, X., and Tong, Y. (2016). Activated carbon fiber paper with exceptional capacitive performance as a robust electrode for supercapacitors. J. Mater. Chem. A *4*, 5828–5833.

70. Gogotsi, Y., and Simon, P. (2011). True performance metrics in electrochemical energy storage. Science *334*, 917–918.

71. Chen, C., Zhang, Y., Li, Y., Dai, J., Song, J., Yao, Y., Gong, Y., Keizewski, L., Xie, J., and Hu, L. (2017). All-wood, low tortuosity, aqueous, biodegradable supercapacitors with ultra-high capacitance. Energy Environ. Sci. *10*, 538–545.

72. Zhang, M., Yu, X., Ma, H., Du, W., Qu, L., Li, C., and Shi, G. (2018). Robust graphene composite films for multifunctional electrochemical capacitors with an ultrawide range of areal mass loading toward high-rate frequency response and ultrahigh specific capacitance. Energy Environ. Sci. *11*, 559–565.

73. Chang, L., Wei, W., Sun, K., and Hu, Y.H. (2017). Excellent performance of highly conductive porous Na-embedded carbon nanowalls for electric double-layer capacitors with a wide operating temperature range. J. Mater. Chem. A *5*, 9090–9096.

74. Sheberla, D., Bachman, J.C., Elias, J.S., Sun, C.J., Horn, Y.S., and Dinca, M. (2017). Conductive MOF electrodes for stable supercapacitors with high areal capacitance. Nat. Mater. *16*, 220–224.

75. Bu, Y., Sun, T., Cai, Y., Du, L., Zhuo, O., Yang, L., Wu, Q., Wang, X., and Hu, Z. (2017). Compressing carbon nanocages by capillarity for optimizing porous structures toward ultrahigh-volumetric-performance supercapacitors. Adv. Mater. *29*, 1700470.

76. Maiti, U.N., Lim, J., Lee, K.E., Lee, W.J., and Kim, S.O. (2014). Three-dimensional shape engineered, interfacial gelation of reduced graphene oxide for high-rate, large capacity supercapacitors. Adv. Mater. *26*, 615–619.

77. Lukatskaya, M.R., Kota, S., Lin, Z., Zhao, M.Q., Shpigel, N., Levi, M.D., Halim, J., Taberna, P.L., Barsoum, M.W., Simon, P., et al. (2017). Ultra-high-rate pseudocapacitive energy storage in two-dimensional transition metal carbides. Nat. Energy *2*, 17105.

78. Zhang, C., Lv, W., Tao, Y., and Yang, Q.H. (2015). Towards superior volumetric performance: design and preparation of novel carbon materials for energy storage. Energy Environ. Sci. *8*, 1390–1403.

79. Ma, H., Zhou, Q., Wu, M., Zhang, M., Yao, B., Gao, T., Wang, H., Li, C., Sui, D., Chen, Y., et al. (2018). Tailoring the oxygenated groups of graphene hydrogels for high-performance supercapacitors with large areal mass loadings. J. Mater. Chem. A *6*, 6587–6594.

80. Cong, H.P., Chen, J.F., and Yu, S.H. (2014). Graphene-based macroscopic assemblies and architectures: an emerging material system. Chem. Soc. Rev. *43*, 7295–7325.

81. Niu, Z., Chen, J., Hng, H.H., Ma, J., and Chen, X. (2012). A leavening strategy to prepare reduced graphene oxide foams. Adv. Mater. *24*, 4144–4150.

82. Zhao, Y., Hu, C., Hu, Y., Cheng, H., Shi, G., and Qu, L. (2012). A versatile, ultralight, nitrogen-doped graphene framework. Angew. Chem. Int. Ed. *51*, 11371–11375.

83. Li, D., Muller, M.B., Gilje, S., Kaner, R.B., and Wallace, G.G. (2008). Processable aqueous dispersions of graphene nanosheets. Nat. Nanotechnol. *3*, 101–105.

84. Marcano, D.C., Kosynkin, D.V., Berlin, J.M., Sinitskii, A., Sun, Z., Slesarev, A., Alemany, L.B., Lu, W., and Tour, J.M. (2010). Improved synthesis of graphene oxide. ACS Nano *4*, 4806–4814.

85. Tung, V.C., Allen, M.J., Yang, Y., and Kaner, R.B. (2009). High-throughput solution processing of large-scale graphene. Nat. Nanotechnol. *4*, 25–29.

86. Guo, H.L., Wang, X.F., Qian, Q.Y., Wang, F.B., and Xia, X.H. (2009). A green approach to the synthesis of graphene nanosheets. ACS Nano *3*, 2653–2659.

87. Xu, Y., Chen, C.Y., Zhao, Z., Lin, Z., Lee, C., Xu, X., Wang, C., Huang, Y., Shair, M.I., and Duan, X. (2015). Solution processable holey graphene oxide and its derived macrostructures for high-performance supercapacitors. Nano Lett. *15*, 4605–4610.

88. Luo, J., Jang, H.D., Sun, T., Xiao, L., He, Z., Katsoulidis, A.P., Kanatzidis, M.G., Gibson, J.M., and Huang, J.X. (2011). Compression and aggregation-resistant particles of crumpled soft sheets. ACS Nano *5*, 8943–8949.

89. Luo, J., Jang, H.D., and Huang, J. (2013). Effect of sheet morphology on the scalability of graphene-based ultracapacitors. ACS Nano *7*, 1464–1471.

90. Kim, T.Y., Jung, G., Yoo, S., Suh, K.S., and Ruoff, R.S. (2013). Activated graphene-based carbons as supercapacitor electrodes with macro- and mesopores. ACS Nano *7*, 6899–6905.

91. Jo, E.H., Choi, J.H., Park, S.R., Lee, C.M., Chang, H., and Jang, H.D. (2016). Size and structural effect of crumpled graphene balls

on the electrochemical properties for supercapacitor application. Electrochim. Acta *222*, 58–63.

92. Mao, S., Wen, Z., Bo, Z., Chang, J., Huang, X., and Chen, J. (2014). Hierarchical nanohybrids with porous CNT-networks decorated crumpled graphene balls for supercapacitors. ACS Appl. Mater. Interfaces *6*, 9881–9889.

93. Li, Z., Gadipelli, S., Yang, Y., and Guo, Z. (2017). Design of 3D graphene-oxide spheres and their derived hierarchical porous structures for high performance supercapacitors. Small *13*, 1702474.

94. Zhao, B., Chen, D., Xiong, X., Song, B., Hu, R., Zhang, Q., Rainwater, B.H., Waller, G.H., Zhen, D., Ding, Y., et al. (2017). A high-energy, long cycle-life hybrid supercapacitor based on graphene composite electrodes. Energy Storage Mater. *7*, 32–39.

95. Lee, C., Jo, E.H., Kim, S.K., Choi, J.H., Chang, H., and Jang, H.D. (2017). Electrochemical performance of crumpled graphene loaded with magnetite and hematite nanoparticles for supercapacitors. Carbon *115*, 331–337.

96. Mao, S., Wen, Z., Kim, H., Lu, G., Hurley, P., and Chen, J. (2012). A general approach to one-pot fabrication of crumpled graphene-based nanohybrids for energy applications. ACS Nano *6*, 7505–7513.

97. Chen, L., Liu, Y., Zhao, Y., Chen, N., and Qu, L. (2016). Graphene-based fibers for supercapacitor applications. Nanotechnology *27*, 032001.

98. Fan, T., Zhao, C., Xiao, Z., Guo, F., Cai, K., Lin, H., Liu, Y., Meng, H., Min, Y., and Epstein, A.J. (2016). Fabricating of high-performance functional graphene fibers for micro-capacitive energy storage. Sci. Rep. *6*, 29534.

99. Pan, H., Wang, D., Peng, Q., Ma, J., Meng, X., Zhang, Y., Ma, Y., Zhu, S., and Zhang, D. (2018). High-performance microsupercapacitors based on bioinspired graphene microfibers. ACS Appl. Mater. Interfaces *10*, 10157–10164.

100. Zhao, X., Zheng, B., Huang, T., and Gao, C. (2015). Graphene-based single fiber supercapacitor with a coaxial structure. Nanoscale *7*, 9399–9404.

101. Yu, J., Wang, M., Xu, P., Cho, S.H., Suhr, J., Gong, K., Meng, L., Huang, Y., Byun, J.H., Oh, Y., et al. (2017). Ultrahigh-rate wire-shaped supercapacitor based on graphene fiber. Carbon *119*, 332–338.

102. Lee, G., Lee, C., Yoon, C.M., Kim, M., and Jang, J. (2017). High-performance three-dimensional mesoporous graphene electrode for supercapacitors using lyophilization and plasma reduction. ACS Appl. Mater. Interfaces *9*, 5222–5230.

103. Duy, L.X., Peng, Z., Li, Y., Zhang, J., and Ji, Y. (2018). Laser-induced graphene fibers. Carbon *126*, 472–479.

104. Cai, W., Lai, T., and Ye, J. (2015). A spinneret as the key component for surface-porous graphene fibers in high energy density micro-supercapacitors. J. Mater. Chem. A *3*, 5060–5066.

105. Huang, G., Hou, C., Shao, Y., Zhu, B., Jia, B., Wang, H., Zhang, Q., and Li, Y. (2015). High-performance all-solid-state yarn supercapacitors based on porous graphene. Nano Energy *12*, 26–32.

106. Li, Z., Huang, T., Gao, W., Xu, Z., Chang, D., Zhang, C., and Gao, C. (2017). Hydrothermally activated graphene fiber fabrics for textile electrodes of supercapacitors. ACS Nano *11*, 11056–11065.

107. Cai, W., Lai, T., Lai, J., Xie, H., Ouyang, L., Ye, J., and Yu, C. (2016). Transition metal sulphides grown on graphene fibers for wearable asymmetric supercapacitors with high volumetric capacitance and high energy density. Sci. Rep. *6*, 26890.

108. Stsikala, S.P., Lee, K.F., Lim, J., Lee, H.J., Koo, S.H., Kim, I.H., Jung, H.J., and Kim, S.O. (2017). Interface-confined high crystalline growth of semiconducting polymers at graphene fibers for high-performance wearable supercapacitors. ACS Nano *11*, 9424–9434.

109. Li, P., Jin, Z., Peng, L., Zhao, F., Xiao, D., Jin, Y., and Yu, G. (2018). Stretchable all-gel-state fiber-shaped supercapacitors enabled by macromolecularly interconnected 3D graphene/nanostructured conductive polymer hydrogels. Adv. Mater. *10*, 1800124.

110. Yang, X., Zhu, J., Qiu, L., and Li, D. (2011). Bioinspired effective prevention of restacking in multilayered graphene films: towards the next generation of high-performance supercapacitors. Adv. Mater. *23*, 2833–2838.

111. Jung, S.M., Mafra, D.L., Lin, C.T., Jung, H.Y., and Kong, J. (2015). Controlled porous structures of graphene aerogels and their effect on supercapacitor performance. Nanoscale *7*, 4386–4393.

112. Tao, Y., Xie, X., Lv, W., Tang, D.M., Kong, D., Huang, Z., Nishihara, H., Ishii, T., Li, B., Golberg, D., et al. (2013). Towards ultrahigh volumetric capacitance: graphene derived highly dense but porous carbons for supercapacitors. Sci. Rep. *3*, 2975.

113. Li, Y., Li, Z., and Shen, P.K. (2013). Simultaneous formation of ultrahigh surface area and three-dimensional hierarchical porous graphene-like networks for fast and highly stable supercapacitors. Adv. Mater. *25*, 2474–2480.

114. Pham, D.T., Lee, T.H., Luong, D.H., Yao, F., Ghosh, A., Le, V.T., Kim, T.H., Li, B., Chang, J., and Lee, Y.H. (2015). Carbon nanotube-bridged graphene 3D building blocks for ultrafast compact supercapacitors. ACS Nano *9*, 2018–2027.

115. Lei, Z., Christov, N., and Zhao, X.S. (2011). Intercalation of mesoporous carbon spheres between reduced graphene oxide sheets for preparing high-rate supercapacitor electrodes. Energy Environ. Sci. *4*, 1866–1873.

116. Wang, W., Guo, S., Penchev, M., Ruiz, I., Bozhilov, K.N., Yan, D., Ozkan, M., and Ozkan, C.S. (2013). Three dimensional few layer graphene and carbon nanotube foam architectures for high fidelity supercapacitors. Nano Energy *3*, 294–303.

117. Song, W.L., Song, K., and Fan, L.Z. (2015). A versatile strategy toward binary three-dimensional architectures based on engineering graphene aerogels with porous carbon fabrics for supercapacitors. ACS Appl. Mater. Interfaces *7*, 4257–4264.

118. Diez, N., Botas, C., Mysyk, R., Goikolea, E., Rojo, T., and Carriazo, D. (2018). Highly packed graphene-CNT films as electrodes for aqueous supercapacitors with high volumetric performance. J. Mater. Chem. A *6*, 3667–3673.

119. Yang, Y., Huang, Q., Niu, L., Wang, D., Yan, C., She, Y., and Zheng, Z. (2017). Waterproof, ultrahigh areal-capacitance, wearable supercapacitor fabrics. Adv. Mater. *29*, 1606679.

120. He, X., Zhang, H., Zhang, H., Li, X., Xiao, N., and Qiu, J. (2014). Direct synthesis of 3D hollow porous graphene balls from coal tar pitch for high performance supercapacitors. J. Mater. Chem. A *2*, 19633–19640.

121. Lin, T., Chen, I.W., Liu, F., Yang, C., Bi, H., Xu, F., and Huang, F. (2015). Nitrogen-doped mesoporous carbon of extraordinary capacitance for electrochemical energy storage. Science *350*, 1508–1513.

122. Wang, X., Zhang, Y., Zhi, C., Wang, X., Tang, D., Xu, Y., Weng, Q., Jiang, X., Mitome, M., Golberg, D., et al. (2013). Three-dimensional strutted graphene grown by substrate-free sugar blowing for high-power-density supercapacitors. Nat. Commun. *4*, 2905.

123. Yu, M., Qiu, W., Wang, F., Zhai, T., Fang, P., Lu, X., and Tong, Y. (2015). Three dimensional architectures: design, assembly and application in electrochemical capacitors. J. Mater. Chem. A *3*, 15792–15823.

124. Tian, X., Jin, J., Yuan, S., Chua, C.K., Tor, S.B., and Zhou, K. (2017). Emerging 3D-printed electrochemical energy storage devices: a critical review. Adv. Energy Mater. *7*, 1700127.

125. Cao, J., He, P., Mohammed, M.A., Zhao, X., Young, R.J., Derby, D., Kinloch, I.A., and Dryfe, R.A.W. (2017). Two-step electrochemical intercalation and oxidation of graphite for the mass production of graphene oxide. J. Am. Chem. Soc. *139*, 17446–17456.

126. Shen, D., Zou, G., Liu, L., Zhao, W., Wu, A., Duley, W.W., and Zhou, Y.N. (2018). Investigation of impact and spreading of molten nanosized gold droplets on solid surfaces. Appl. Opt. *57*, 2080–2086.

127. Cao, Y., Fatemi, V., Demir, A., Fang, S., Tomarken, S.L., Luo, J.Y., Sanchez-Yamagishi, J.D., Watanabe, K., Taniguchi, T., Kaxiras, E., et al. (2018). Correlated insulator behavior at half-filling in magic-angle graphene superlattices. Nature *556*, 80–84.

128. Cao, Y., Fatemi, V., Fang, S., Watanabe, K., Taniguchi, T., Kaxiras, E., and Jarillo-Herrero, P. (2018). Unconventional superconductivity in magic-angle graphene superlattices. Nature *556*, 43–50.

129. Wu, Z., Li, L., Yan, J.M., and Zhang, X.B. (2017). Materials design and system

construction for conventional and new-concept supercapacitors. Adv. Sci. *4*, 1600382.

130. Dubal, D.P., Chodankar, N.R., Kim, D.H., and Gomez-Romero, P. (2018). Towards flexible solid-state supercapacitors for smart and wearable electronics. Chem. Soc. Rev. *47*, 2065–2129.

131. Wang, F., Wu, X., Yuan, X., Liu, Z., Zhang, Y., Fu, L., Zhu, Y., Zhou, Q., Wu, Y., and Huang, W. (2017). Latest advances in supercapacitors: from new electrode materials to novel device designs. Chem. Soc. Rev. *46*, 6816–6854.

132. Graphene-info. (2019). ZapGo. https://www.graphene-info.com/zap-go.

133. Skeleton Technologies. (2019). Largest ultracapacitor manufacturer in Europe. https://www.skeletontech.com/investors.

134. SupercapTech.com. (2019). Graphene supercapacitors 2.8 V 30000 F and 3 V 12000 F made in China. https://www.supercaptech.com/graphene-supercapacitors-2-8v-30000f-and-3v-12000f-made-in-china.